ornl

ORNL-5840



ORNL--5840

DE82 012960

OAK
RIDGE
NATIONAL
LABORATORY

UNION
CARBIDE

# Chemical Composition Effects on the Creep of Austenitic Stainless Steel Weld Metals

R. L. Klueh
D. P. Edmonds

METALS and CERAMICS
ENERGY
RESEARCH
DEVELOPMENT
OAK RIDGE NATIONAL LABORATORY



OPERATED BY
UNION CARBIDE CORPORATION
FOR THE UNITED STATES
DEPARTMENT OF ENERGY

---

ORNL-5840
Distribution
Categories
UC-79Th, -Tk, -Tr
OR 1.4 Fabrication
Technology

Contract No. W-7405-eng-26

METALS AND CERAMICS DIVISION

# CHEMICAL COMPOSITION EFFECTS ON THE CREEP OF AUSTENITIC STAINLESS STEEL WELD METALS

R. L. Klueh and D. P. Edmonds



Date Published - May 1982

Prepared by
OAK RIDGE NATIONAL LABORATORY
Oak Ridge, Tennessee 37830
operated by
UNION CARBIDE CORPORATION
for the
DEPARTMENT OF ENERGY

CONTENTS

# CHEMICAL COMPOSITION EFFECTS ON THE CREEP OF AUSTENITIC STAINLESS STEEL WELD METALS*

R. L Klueh and D. P. Edmonds

ABSTRACT

Alloying additions of titanium, boron, and phosphorus are known to affect the elevated-temperature strength and ductility of austenitic stainless steel weld metals. We studied the effect of these elements on the creep-rupture properties of type 308 stainless steel, type 316 stainless steel, and 16-8-2 weld metals. Creep-rupture tests were made at 649°C on specimens taken from gas tungsten arc welds deposited by use of commercial and experimental weld filler wires. Additions of about 0.4 and 0.8% Ti to the commercial composition for type 308 stainless steel increased its strength and ductility over those of welds made with a commercial filler wire. A maximum in the effect of titanium was apparent: the 0.4% Ti alloy had better strength and ductility. Although small additions of boron and phosphorus had only a minor effect on strength and ductility when added to the commercial composition separately or in combination, the addition of approximately 0.006% B and 0.042% P to a 0.4% Ti alloy significantly increased its strength above that of the 0.4% Ti alloy without boron and phosphorus. A similar effect of titanium was observed for type 316 stainless steel: boron and phosphorus additions had little effect on strength and ductility above the effect of the optimum titanium additions. The results for the type 16-8-2 weld metal were not as unequivocal. Although additions of titanium and titanium plus boron and phosphorus again favorably affected the strength and ductility, there were significant strength variations among the welds.

The microstructures of the welds were examined, and the differences were characterized in terms of the δ-ferrite morphologies. Although the microstructures of the weld metals were significantly different from comparable base-metal compositions, the effect of titanium on strength in the weld was similar to the effect of titanium in austenitic stainless steel base metals (with no δ-ferrite). Similar observations were made on the effects of boron and phosphorus. Possible explanations of these effects are proposed.

---

*Work performed under DOE/RRT AF 15 40 10.3, Task OR-1.4, Fabrication Technology.

# INTRODUCTION

Stress-rupture fractures of austenitic stainless steel weld metals often occur with quite low ductilities. As a result, *ASME Pressure Vessel and Piping Code* Case N-47 allows only one-half the deformation allowed for similar wrought alloys. Furthermore, the creep-rupture strengths of weld metals are often less than those of wrought base metals with similar compositions.

Over the past several years, ORNL has conducted a research program to develop appropriate weld metals with improved strength and ductility.[1–4] Initial work on type 308 shielded metal arc welds showed that titanium from titania and lime-titania electrodes favorably affected the creep-rupture properties.[1,2] Special electrodes, prepared by a commercial manufacturer, were used to study chemical composition effects on type 308 stainless steel weld metal.

The results of these studies indicated that[1,2]

1. an increased carbon concentration caused an increase in creep-rupture strength and a decrease in ductility,
2. a reduction in silicon caused an increase in ductility with little effect on strength,
3. an increase in phosphorus caused an increase in rupture life and an improvement in ductility,
4. sulfur had little effect on properties, and
5. an increase in boron increased rupture life and ductility.

Results on shielded metal arc type 316 stainless steel welds indicated similar chemical composition effects. These studies led to the development of controlled residual element (CRE) electrodes that yield weld metal deposits with nominally 0.05% Ti, 0.04% P, and 0.006% B.

In this report we describe efforts to determine optimum compositions for gas tungsten arc (GTA) welding wire. Studies on the effect of chemical composition on mechanical properties and microstructure were conducted in an effort to understand the strengthening mechanisms involved so that, if possible, these mechanisms can be applied to other alloy systems and welds made by other processes.

## EXPERIMENTAL

Small experimental heats of types 308, 316, and 16-8-2 stainless steel were melted, cast, and fabricated into 3.2-mm-diam weld filler wire. Selected additions of P, B, Si, and Ti were made to these heats to determine the effect of these elements on the creep-rupture behavior and ductility of the weld metal.

All the test welds were made in 13-mm-thick stainless steel plates by use of a 75°-included-angle V-groove joint. The type 308 stainless steel welds were made in type 304 plates, and the type 316 and 16-8-2 welds were made in type 316 plates. The welds were made by the manual GTA process and stringer-bead techniques with average welding conditions of 190-A current and 17 V [direct current straight polarity (DCSP)]. All welds used pure argon shielding gas.

All-weld-metal buttonhead specimens with a 3.2-mm-diam by 28.6-mm-long gage section parallel to the welding direction were machined from each test weld. The center of each specimen coincided with the middle of the weld about 5 mm below the top surface of the weld. These specimens were tested at 649°C in air at stress levels intended to produce rupture times from 10 to 100 to several thousand hours. The load was applied gradually by mechanical and/or hydraulic devices. Extensometers mounted on the grips were used to monitor creep strains to within ±1%, with the total elongation and reduction of area being measured directly by fitting the fractured specimens together. Rupture data only are considered in this report.

## RESULTS

Because Ti, Si, B, and P proved important in previous studies on shielded metal arc welds, we examined their effect on manual GTA welds made with experimental heats of type 308 stainless steel, type 316 stainless steel, and 16-8-2 filler wire. Tables 1 through 3 give the chemical compositions of the heats tested. For each of the experimental heats we determined a creep-rupture curve at 649°C. Results for each type of the filler metals are presented separately.

Table 1. Chemical composition of experimental type 308 stainless steel filler metal

| Weld | Filler metal[a] | Deposit composition, wt % | | | | | | | | | | | | | | |
|---|---|---|---|---|---|---|---|---|---|---|---|---|---|---|---|---|
| | | Cr | Ni | Mo | C | B | P | Ti | Si | S | Mn | Co | Cu | Cb | Ta | N |
| V-6 | Commercial heat D1773081 | 21.2 | 9.8 | 0.17 | 0.024 | 0.0005 | 0.018 | <0.02 | 0.58 | 0.015 | 1.55 | <0.05 | 0.05 | <0.05 | 0.1 | 0.038 |
| V-14 | Commercial remelt | 21.5 | 9.9 | 0.02 | 0.026 | 0.007 | 0.013 | <0.01 | 0.48 | 0.008 | 1.59 | 0.02 | 0.06 | <0.01 | | |
| V-10 | No Si | 21.5 | 9.9 | 0.04 | 0.026 | 0.002 | 0.035 | <0.01 | 0.02 | 0.027 | 1.95 | 0.01 | <0.01 | <0.01 | | |
| V-11 | 0.60% Si | 21.5 | 10.0 | 0.03 | 0.026 | 0.002 | 0.025 | <0.01 | 0.58 | 0.026 | 1.88 | 0.01 | <0.01 | <0.01 | | |
| V-8 | 0.007% B[b] | 21.7 | 10.0 | 0.02 | 0.029 | 0.003 | 0.012 | <0.01 | 0.49 | 0.008 | 1.58 | 0.02 | 0.06 | <0.01 | | 0.037 |
| V-13 | 0.015% B[b] | 21.5 | 9.9 | 0.02 | 0.026 | 0.007 | 0.013 | <0.01 | 0.48 | 0.008 | 1.59 | 0.02 | 0.06 | <0.01 | | |
| V-12 | 0.045% P | 21.5 | 9.9 | 0.02 | 0.026 | 0.001 | 0.045 | <0.01 | 0.48 | 0.008 | 1.58 | 0.02 | 0.05 | <0.01 | | |
| V-9 | 0.06% P | 21.3 | 9.9 | 0.02 | 0.038 | 0.001 | 0.049 | <0.01 | 0.48 | 0.008 | 1.59 | 0.02 | 0.12 | <0.01 | | 0.038 |
| V-16 | 0.045% P, 0.007% B[b] | 21.5 | 9.9 | 0.01 | 0.026 | 0.003 | 0.051 | <0.01 | 0.50 | 0.008 | 1.55 | 0.02 | 0.05 | <0.01 | | |
| V-15 | 0.5% Ti | 21.5 | 9.9 | 0.02 | 0.026 | 0.001 | 0.012 | 0.49 | 0.52 | 0.008 | 1.55 | 0.02 | 0.05 | <0.01 | | |
| V-7 | 1.0% Ti[b] | 21.3 | 10.1 | 0.03 | 0.033 | 0.001 | 0.012 | 0.88 | 0.55 | 0.008 | 1.56 | 0.02 | 0.06 | 0.01 | | 0.039 |
| V-130 | 0.042% P, 0.006% B, 0.5% Ti | 21.1 | 10.1 | 0.05 | 0.028 | 0.006 | 0.041 | 0.47 | 0.58 | 0.008 | 1.57 | | | | | |

[a]Nominal intended compositions.

[b]Actual composition was less than aim.

Table 2. Chemical composition of experimental type 316 stainless steel filler metal

| Weld | Filler metal[a] | Chemical composition, wt % | | | | | | | | | | | | | | |
|---|---|---|---|---|---|---|---|---|---|---|---|---|---|---|---|---|
| | | Cr | Ni | Mo | C | B | P | Ti | Si | S | Mn | Co | Cu | Cb | Ta | N |
| V-1,2 | Commercial | 18.9 | 13.0 | 2.2 | 0.044 | 0.0004 | 0.023 | <0.02 | 0.044 | 0.013 | 1.75 | 0.1 | 0.09 | <0.05 | <0.1 | 0.033 |
| V-44 | 0.3% Ti | 17.5 | 14.0 | 2.5 | 0.047 | <0.0005 | 0.005 | 0.29 | 0.03 | 0.004 | 1.41 | 0.018 | 0.01 | <0.005 | <0.015 | 0.003 |
| V-123, 124 | 0.5% Ti[b] | 18.7 | 13.0 | 2.3 | 0.047 | 0.001 | 0.028 | 0.36 | 0.54 | 0.001 | 1.71 | | | | | |
| V-126, 128 | 1.0% Ti[b] | 18.1 | 13.1 | 2.2 | 0.055 | 0.001 | 0.021 | 0.83 | 0.58 | 0.012 | 1.72 | 0.17 | 0.14 | 0.03 | | 0.030 |
| V-116, 117 | 0.006% B, 0.042% P | 18.8 | 13.0 | 2.4 | 0.039 | 0.007 | 0.050 | 0.01 | 0.51 | 0.012 | 1.74 | | | | | |
| V-122, 129 | 0.006% B, 0.042% P, 0.5% Ti[b] | 18.6 | 13.0 | 2.3 | 0.047 | 0.006 | 0.046 | 0.37 | 0.54 | 0.011 | 1.73 | | | | | |

[a]Nominal intended compositions.

[b]Actual composition was less than aim.

Table 3. Chemical composition of experimental 16-8-2 filler metal

| Weld | Filler metal[a] | Chemical composition, wt % | | | | | | | | | | | | | | |
|---|---|---|---|---|---|---|---|---|---|---|---|---|---|---|---|---|
| | | Cr | Ni | Mo | C | B | P | Ti | Si | S | Mn | Co | Cu | Cb | Ta | N |
| V-86 | Commercial | 15.16 | 8.43 | 1.28 | 0.07 | 0.001 | 0.019 | 0.01 | 0.42 | 0.011 | 1.44 | | | | | |
| V-115 | Commercial | 15.96 | 8.79 | 1.62 | 0.049 | | 0.027 | | 0.26 | 0.010 | 1.17 | | | | | |
| V-121 | 0.006% B, 0.042% P[b] | 15.94 | 7.43 | 1.76 | 0.050 | 0.003 | 0.034 | 0.01 | 0.09 | 0.011 | 1.62 | 0.07 | 0.10 | 0.02 | | 0.032 |
| V-118 | 0.5% Ti[b] | 15.50 | 7.20 | 1.75 | 0.054 | 0.001 | 0.018 | 0.39 | 0.09 | 0.011 | 1.60 | | | | | |
| V-125 | 0.5% Ti[b] | 15.41 | 7.73 | 1.76 | 0.058 | 0.001 | 0.018 | 0.36 | 0.23 | 0.013 | 1.70 | 0.12 | 0.11 | 0.03 | | 0.029 |
| V-119 | 1.0% Ti[b] | 15.15 | 7.28 | 1.75 | 0.060 | 0.001 | 0.019 | 0.78 | 0.009 | 0.011 | 1.57 | | | | | |
| V-127 | 1.0% Ti[b] | 14.97 | 7.71 | 1.75 | 0.062 | 0.001 | 0.018 | 0.79 | 0.21 | 0.012 | 1.66 | 0.11 | 0.10 | 0.03 | | 0.023 |
| V-132 | 0.006% B, 0.042% P, 0.5% Ti[b] | 15.24 | 7.67 | 1.76 | 0.058 | 0.004 | 0.036 | 0.39 | 0.013 | 0.013 | 1.70 | 0.08 | 0.10 | 0.02 | | 0.023 |

[a]Nominal intended compositions.

[b]Actual composition was less than aim.

## Type 308 Stainless Steel

Of the three weld metals studied, we examined type 308 stainless steel in the greatest detail. A stress-rupture curve was determined for type 308 stainless steel weld metal deposited from a commercial heat of filler wire (Fig. 1). Some of this wire was also remelted and fabricated by the same techniques used to compare the experimental heats. We found little difference in the strength [Fig. 1(a)] and ductility [Fig. 1(b)] of the commercial weld deposit before and after remelting.

Initial tests indicated that the 0.05% Ti level that had a significant effect on the strength and ductility of the shielded metal arc welds had little effect on the GTA welds. As a result, type 308 stainless steel weld deposits with nominally 0.5 and 1.0% Ti additions (the 1% alloy contained 0.9% Ti) were obtained and tested. Tests were also made on type 308 stainless steel weld metal with essentially no silicon and with 0.6% Si.

The beneficial effects of titanium were obvious: both the strength and ductility were significantly improved over those of the commercial steel (Fig. 2). The strength and ductility values of the 0.5% Ti alloy were better than those of the 0.9% Ti material. Silicon had little effect on either strength or ductility. The strength of the welds with and without silicon additions fell slightly below the weld deposited with the commercial filler wire, whereas the ductility (even with 0.6% Si) was better than that of the commercial deposits (Fig. 2).

We determined the effects of boron and phosphorus relative to the commercial alloy (Fig. 3) and found that the strength and ductility improvements were much less than those obtained with titanium additions. The combination of boron and phosphorus led to the strongest and most ductile material for the long-time tests of the alloys with only boron and phosphorus added (Fig. 3).

The above results indicated that titanium and the combination of boron and phosphorus have favorable effects on creep-rupture strength and ductility at 649°C. These elements were combined in a heat that contained approximately 0.5% Ti, 0.006% B, and 0.041% P. This alloy was considerably stronger than the alloys doped with only titanium or with 0.006% B and

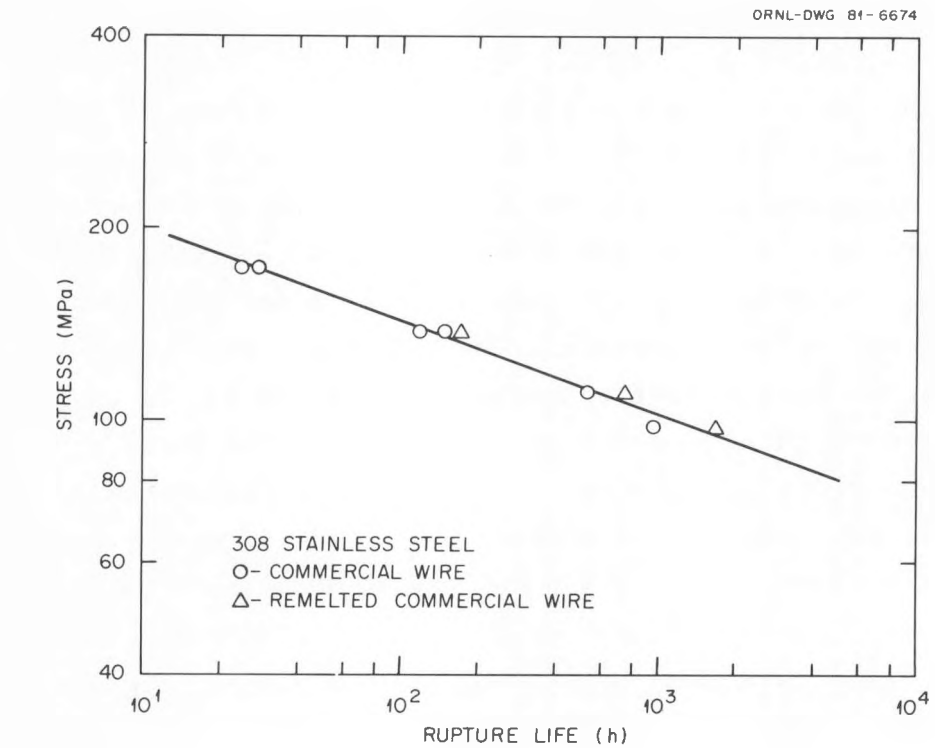


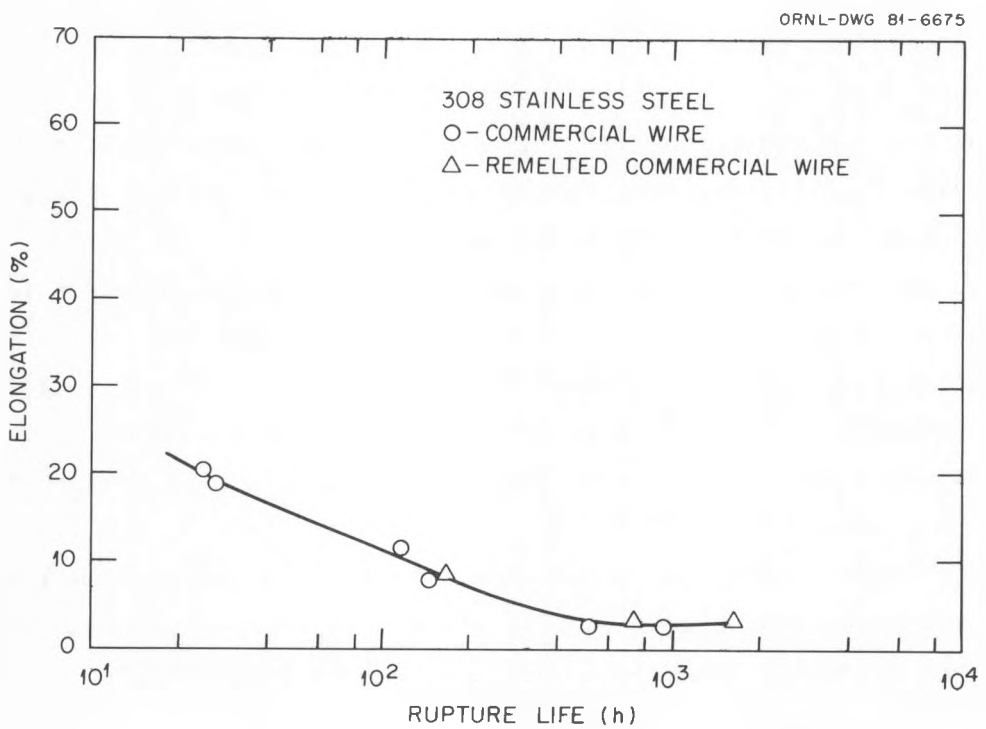


Fig. 1. Commercial type 308 stainless steel weld metal tested at 649° C. (a) Stress-rupture curve. (b) Total elongation plotted against rupture life.

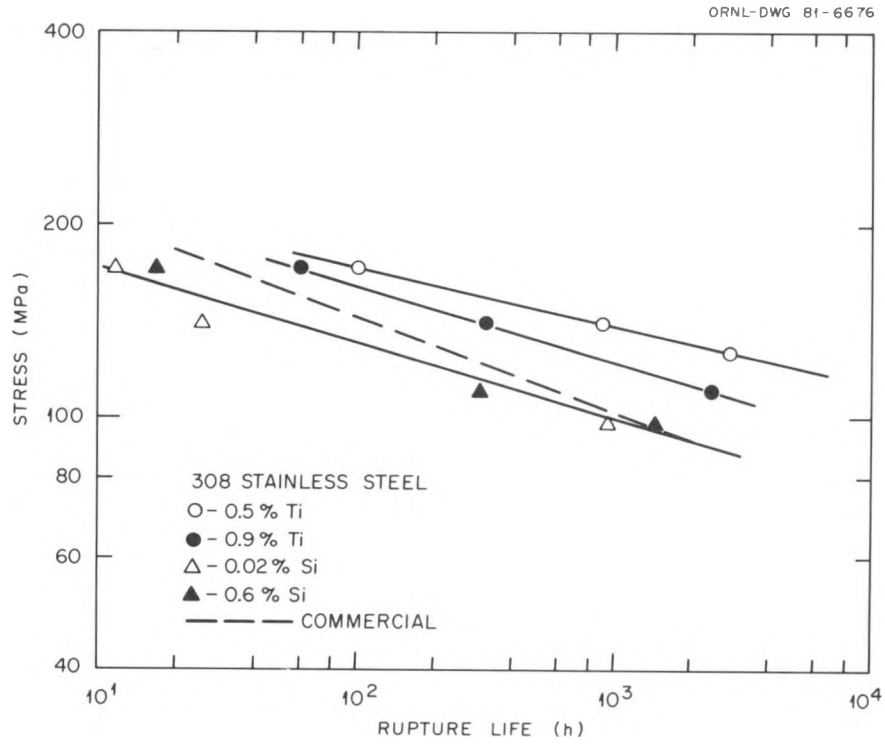


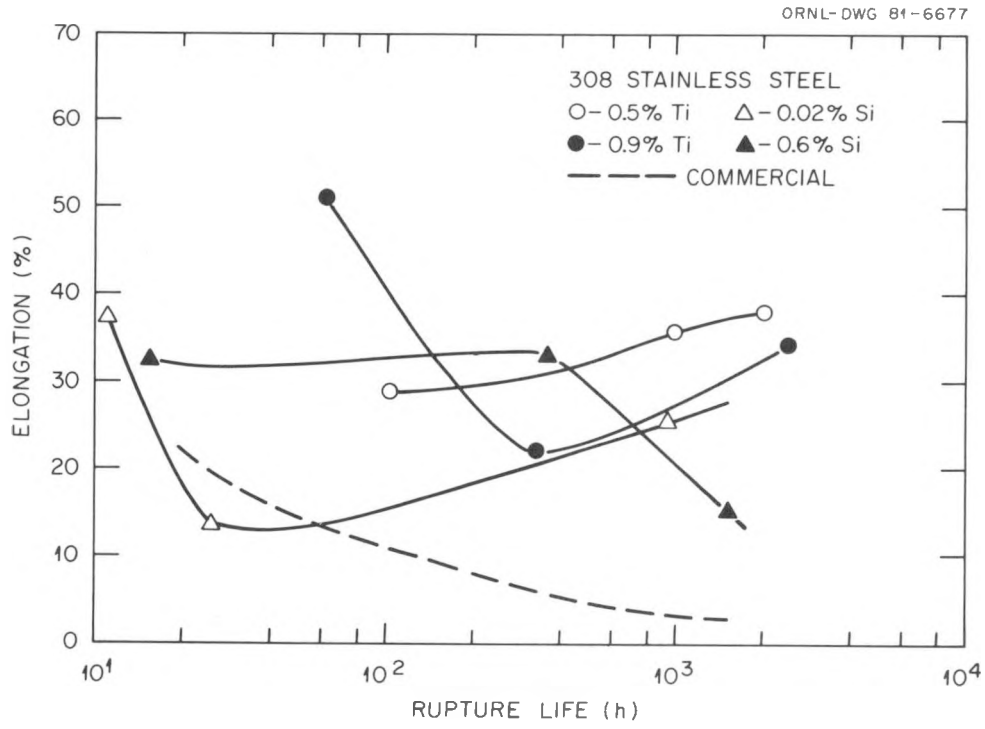


Fig. 2. Experimental heats of type 308 stainless steel weld metal with silicon and titanium additions tested at 649°C. (a) Stress-rupture curves. (b) Total elongation plotted against rupture life.

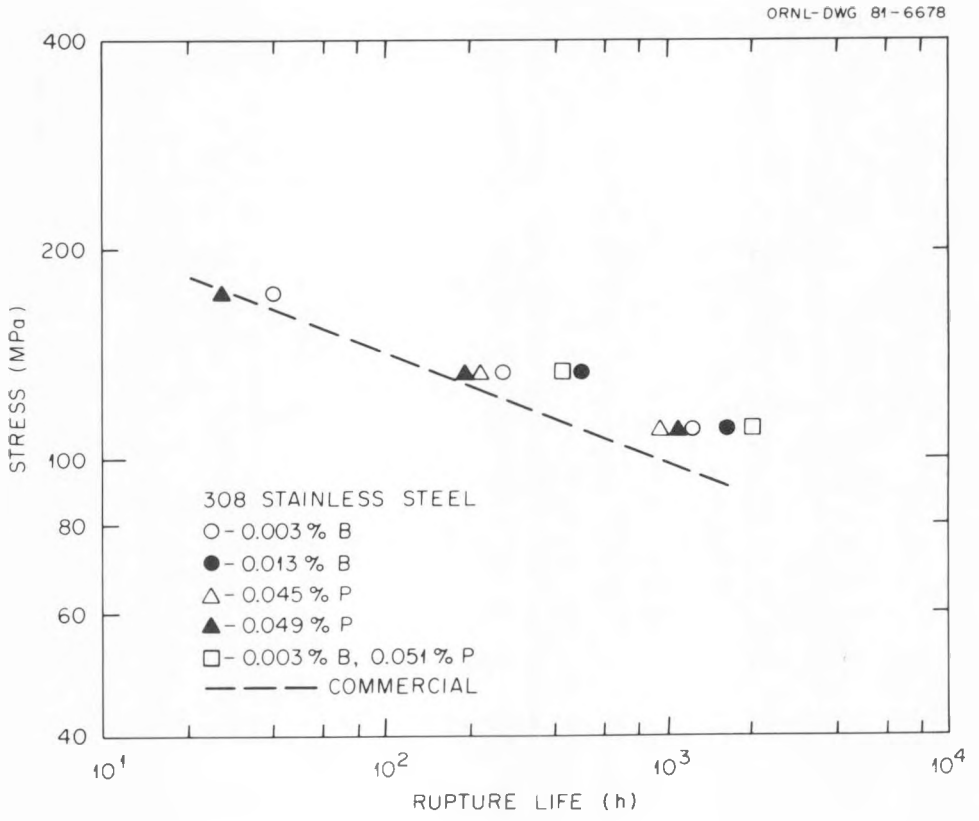


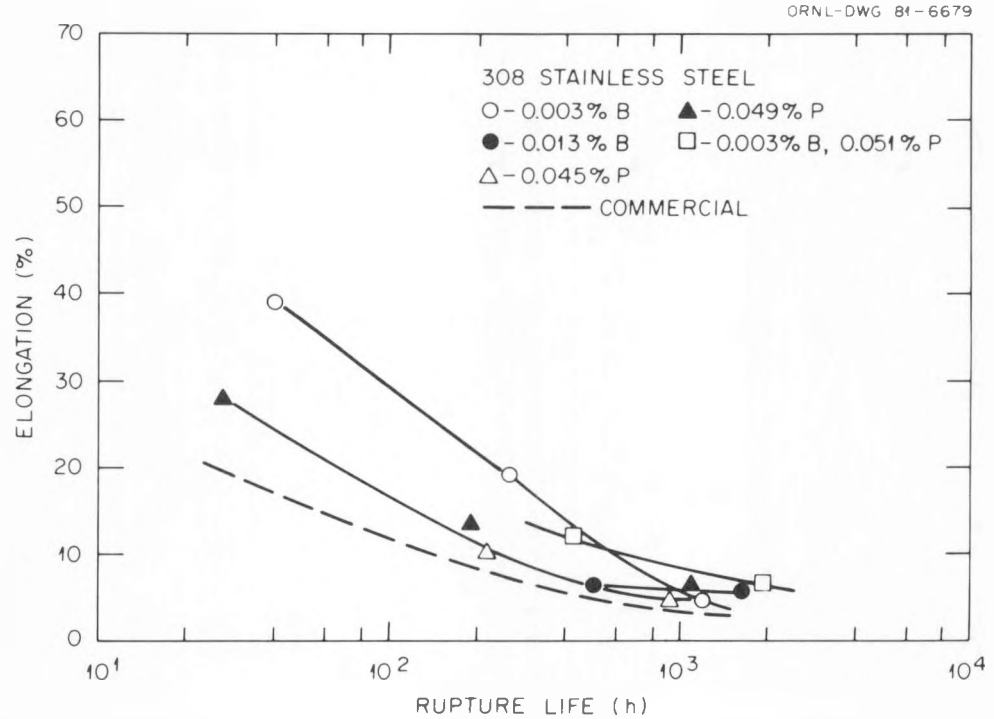


Fig. 3. Experimental heats of type 308 stainless steel weld metal with boron and phosphorus additions tested at 649°C. (a) Stress-rupture data. (b) Total elongation plotted against rupture life.

0.041% P (Fig. 4). The ductility varied considerably [Fig. 4(b)]; however, even for the 3000-h test, the elongation was almost 4 times that of the commercial alloy.

Visual examination of the fractured specimens was in agreement with the ductility measurements. The specimens from the welds made with the commercial filler metals (as received and remelted) had flat fractures (little or no neck formation). On the specimens from the welds made with the as-received commercial filler wire, we found indications of cracks on the external surface. The specimens with nominally 0.02 and 0.6% Si were quite ductile and necked during deformation and fracture. All the low-silicon specimens showed considerable necking at all stresses, but the amount of necking decreased with decreasing stress for the 0.6% Si specimens.

All fractures for the welds made with the alloys to which boron and phosphorus were added separately were quite flat (no neck formation). For the specimens from the weld containing 0.045% P and 0.003% B, we found a small amount of necking for the high-stress test but essentially none at the lowest stress.

The fractured specimens from the welds with the titanium additions displayed considerable ductility. All the 0.5 and 0.9% Ti alloy specimens tested necked during fracture. For the specimens of the weld metal that contained 0.041% P, 0.006% B, and 0.5% Ti, all specimens necked, although the necking decreased with decreasing stress. The amount of necking was less than that for specimens from welds having only titanium added.

The ferrite content of the different welds was determined with a ferrite scope on as-welded material and after exposure in a creep test at 649°C (Table 4). The latter measurements were made on the buttonheads of selected creep-test specimens. With a few exceptions, the ferrite number was approximately 12 to 13. Exceptions were the silicon heats, which had somewhat lower values (near 9), and the titanium heats and the heat with boron, phosphorus, and titanium added, for which larger values were obtained (18 to 23).

If the chemical compositions of the alloys are examined (Table 1), the only way to account for the difference in ferrite number for the silicon alloys is the fact that both of these heats contain somewhat more

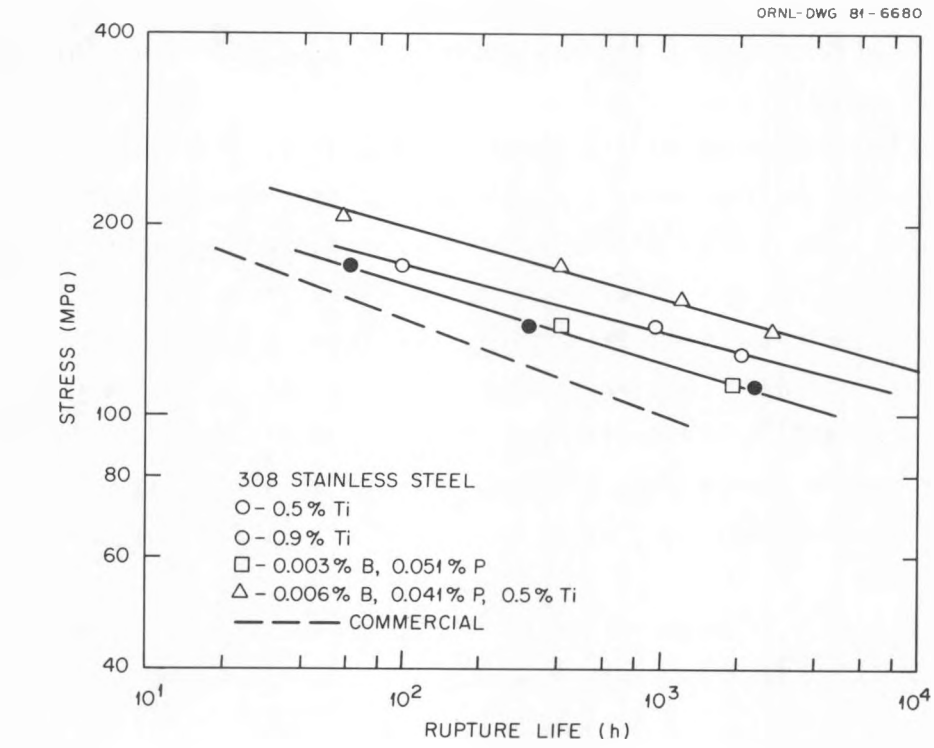


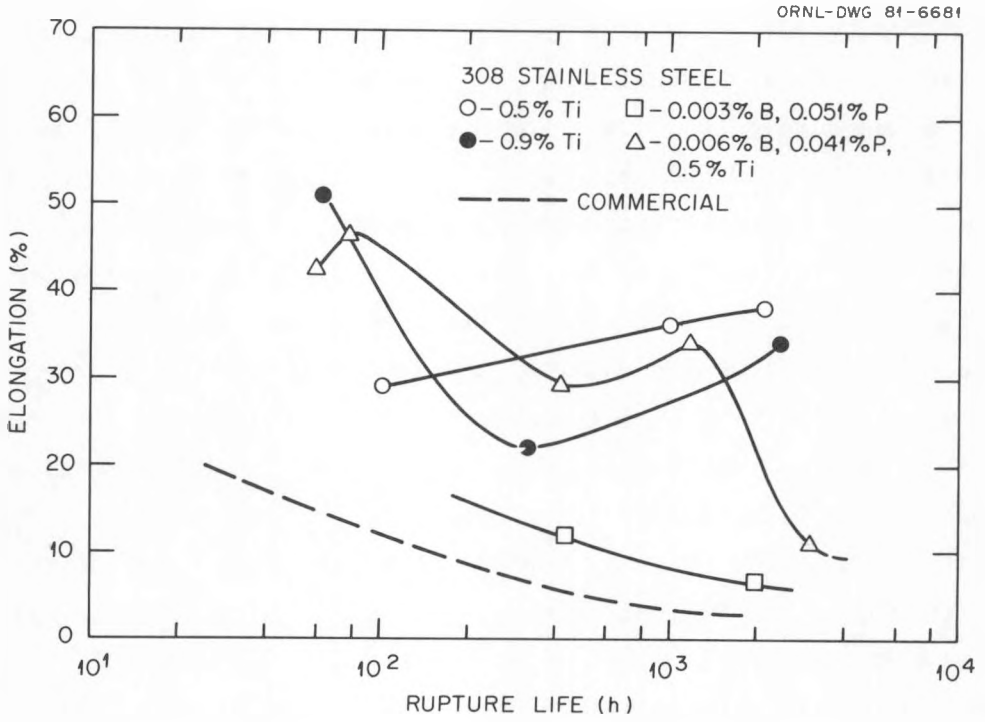


Fig. 4. Experimental heats of type 308 stainless steel weld metal with different combinations of boron, phosphorus, and titanium tested at 649°C. (a) Stress-rupture curves. (b) Total elongation plotted against rupture life.

Table 4. Ferrite number for type 308 stainless steel experimental welds

| Weld | Average ferrite number | |
|---|---|---|
| | As welded | After creep tests[a] |
| Commercial (V-6) | 13.0 | 0.5 (927) |
| Commercial remelt (V-14) | 13.0 | 0.8 (2084) |
| No Si (V-10) | 9.1 | 0.9 (937) |
| 0.6% Si (V-11) | 9.7 | 0.2 (1497) |
| 0.003% B (V-8) | 12.3 | 0.4 (1199) |
| 0.013% B (V-13) | 11.9 | 0.3 (1655) |
| 0.045% P (V-12) | 12.5 | 0.1 (9221) |
| 0.049% P (V-9) | 12.3 | 0.2 (1092) |
| 0.051% P, 0.003% B (V-16) | 12.8 | 0.1 (1980) |
| 0.5% Ti (V-15) | 20.9 | 0.2 (2084) |
| 0.9% Ti (V-7) | 23.9 | 1.3 (321) |
| 0.006% B, 0.041% P, 0.5% Ti (V-130, 131) | 17.8 | 2.4 (34), 0.2 (1708) |

[a]Number in parentheses is duration (h) of creep test for specimen from which the ferrite number was determined.

manganese than the other alloys (manganese is an austenite-stabilizing element). The high ferrite numbers of the two titanium alloys can be attributed to titanium, a ferrite-forming element (titanium also ties up carbon and nitrogen, austenite formers). The reason for the lower ferrite number for the alloy with boron, phosphorus, and titanium additions as compared with the alloys to which only titanium had been added is not immediately obvious, although the difference is probably attributable to boron (boron is an austenite former, phosphorus a ferrite former; a small effect of boron, relative to the commercial alloy, is seen in Table 4, whereas there is little effect from the phosphorus).

The decrease in ferrite number after testing is attributable to the transformation of the unstable ferrite to austenite, nonmagnetic intermetallic phases, and nonmagnetic carbides.[5] Table 4 shows that the decrease in ferrite number depends on the amount of time the creep specimen was at 650°C.

When the weld microstructures were examined, minor differences were detected in substructures (Figs. 5 and 6). The welds were first etched

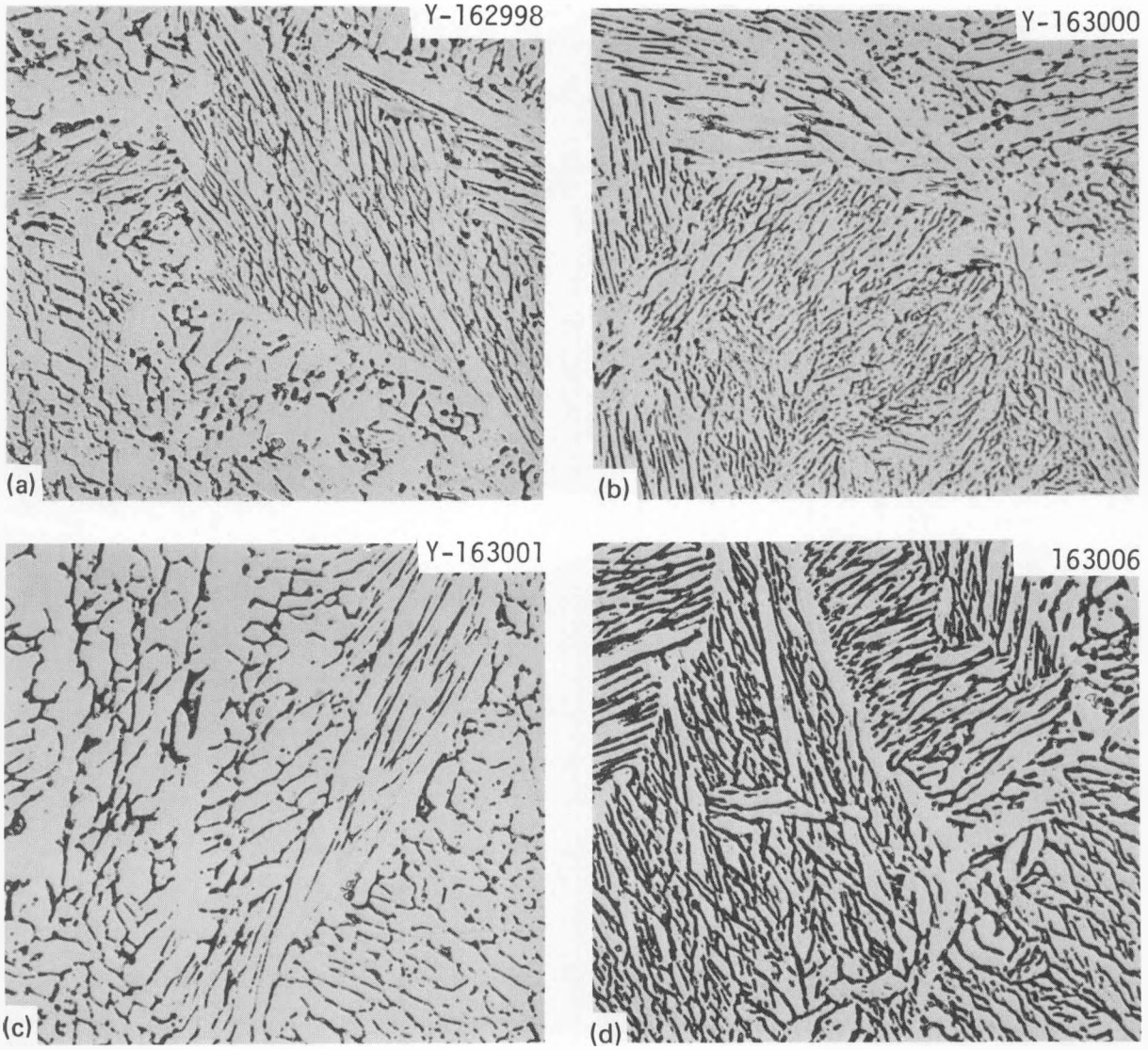


Fig. 5. Microstructures of type 308 stainless steel weld metals. (a) Commercial. (b) 0% Si. (c) 0.6% Si. (d) 0.003% B and 0.051% P.

with an etchant that attacks the polished surface in such a way that ferrite, austenite, sigma phase, and carbides can be distinguished (the etching solution is 15 g $K_4Fe(CN)_6$, 15 g KOH, and 100 mL $H_2O$ and is commonly known as Murakami's etchant). The specimens were then etched with aqua regia (five parts concentrated HCl to one part concentrated $HNO_3$) to bring out the general microstructure. The microstructures revealed by the two etchants are similar, although the aqua regia etch attacks the surface

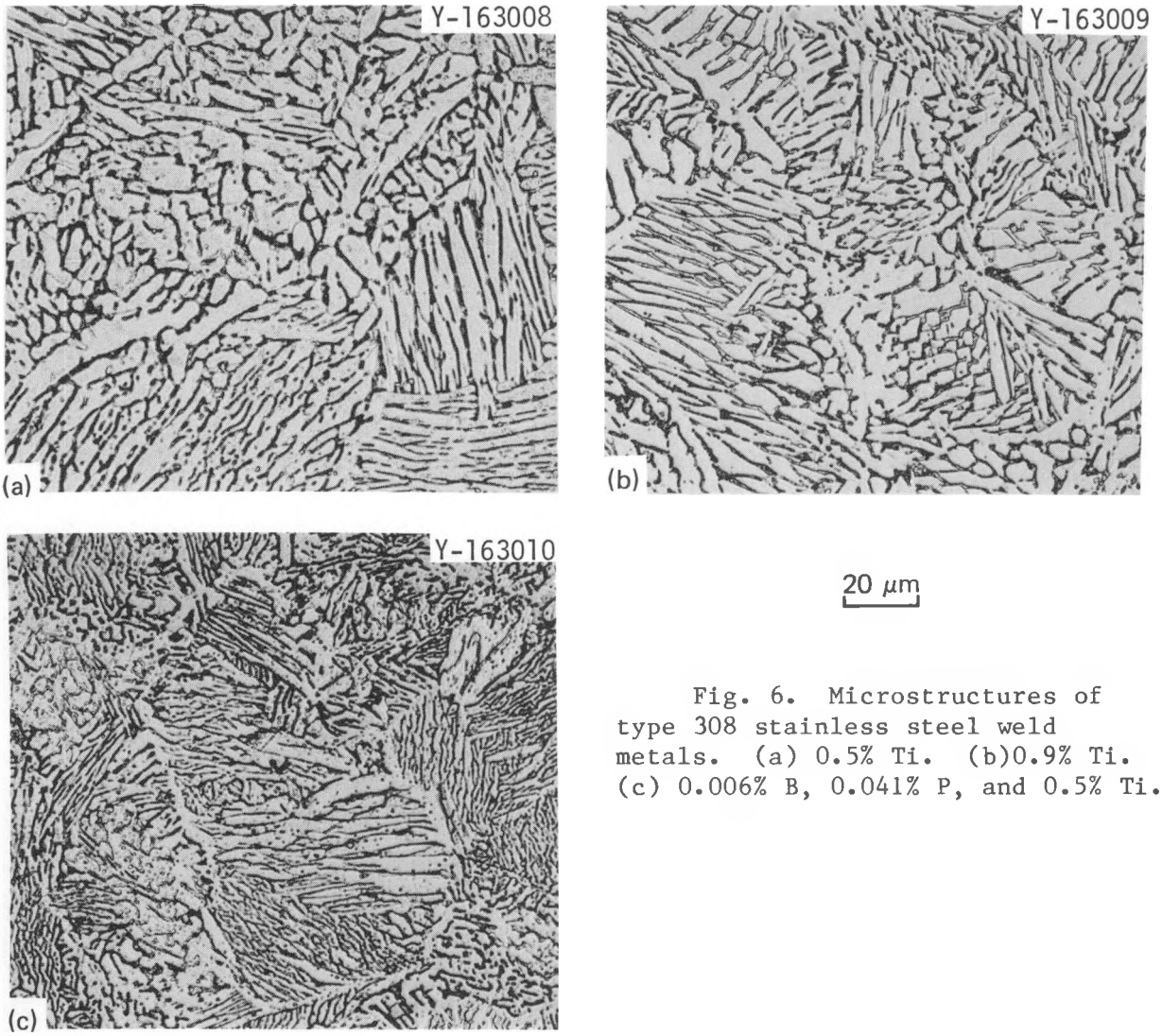


Fig. 6. Microstructures of type 308 stainless steel weld metals. (a) 0.5% Ti. (b)0.9% Ti. (c) 0.006% B, 0.041% P, and 0.5% Ti.

more severely and may tend to give an impression that more δ-ferrite is present than actually is. The discussion of the microstructures will assume that primarily austenite and δ-ferrite were present. This ignores the fact that for such multipass welds, some of the δ-ferrite can transform to an intermetallic phase such as sigma.

Most of the ferrite in the alloys formed as laths or needles (the dark-etching phase in Figs. 5 and 6). However, the regions containing the lath structure were usually surrounded by a narrow zone of light-etching austenite. Along with the difference in ferrite content for the different

welds, the increase in ferrite content appeared to lead to a finer overall microstructure (Fig. 7); that is, the lath spacing and the size of the lath regions surrounded by austenite both decreased.

A close examination of the as-welded microstructures indicates little or no precipitate within the austenite regions (light-etching areas of Fig. 7) of the alloys to which only titanium was added. The alloy that contained titanium, boron, and phosphorus showed some indication of precipitation [Fig. 6(c)]. This could mean that boron and/or phosphorus somehow affect the precipitation of titanium-rich compounds. If true, it would also explain the finer microstructure of this alloy as well as the lower ferrite number (i.e., precipitation removed the ferrite-forming titanium from solution). The boron and phosphorus, either by themselves or together, had little effect on the ferrite number relative to the commercial alloy (Table 4).

The fracture morphologies of the different weld metal specimens reflected the difference in ductility and fracture modes. Inter-substructural cracking was present in the as-received commercial alloy and

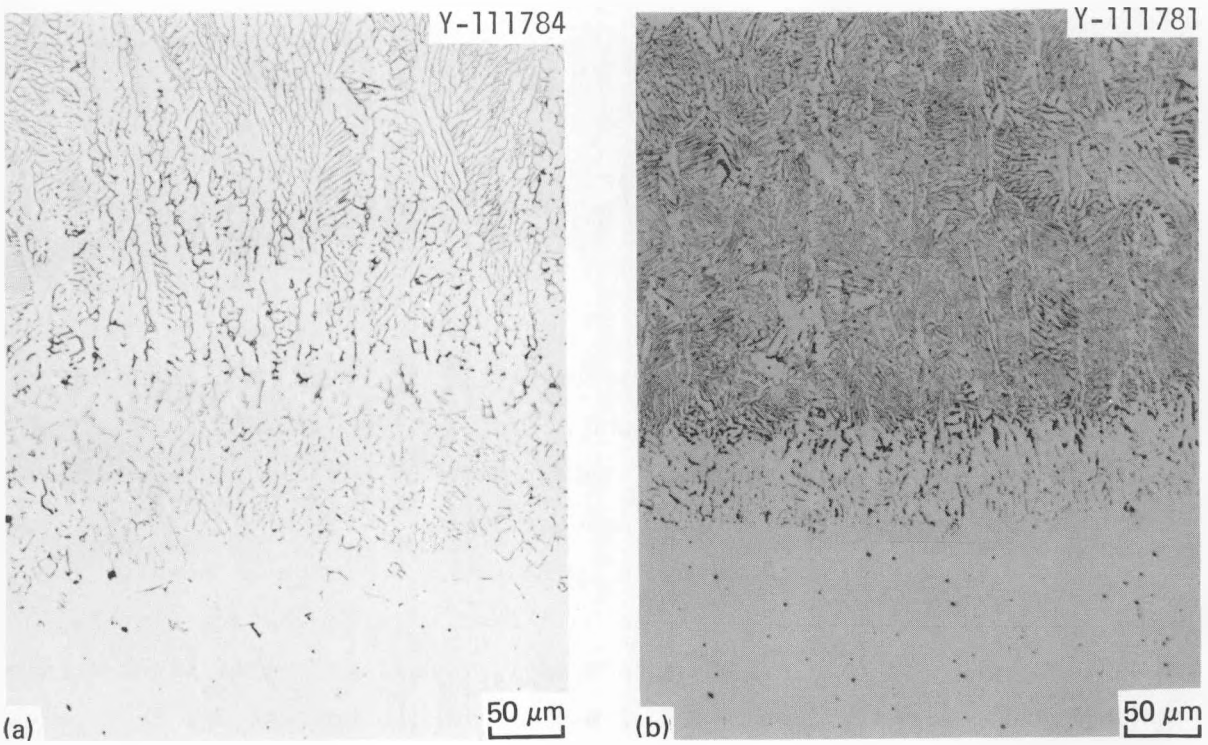


Fig. 7. Comparison of the difference in microstructures of type 308 stainless steel with (a) low and (b) high δ-ferrite content. (a) 0% Si alloy. (b) 0.9% Ti alloy. Weld metal and base metal are shown.

after remelting (Fig. 8). The alloy with a 0.6% Si addition contained somewhat more intersubstructural cracking than without silicon [Figs. 9(a) and 9(b)], although the nature of the cracks was similar. Both the alloys to which boron and phosphorus had been added separately displayed fairly flat fractures with intersubstructural cracking (Fig. 10). An increase in boron concentration from 0.003 to 0.007% (the intended chemistry was 0.007 and 0.015%, respectively) resulted in a decreased amount of crack formation. Considerable crack formation also occurred in the two alloys to which phosphorus had been added (0.045 and 0.049% P). However, all these alloys displayed significant amounts of cracking (Fig. 10). The alloy with both boron and phosphorus additions showed relatively little cracking, although the fractures were quite flat (Fig. 11).

Highly ductile fractures were observed for the steels with approximately 0.5 and 0.9% Ti (Fig. 12). There appeared to be some crack formation in the steel with 0.5% Ti [Fig. 12(a)]. The steel with 0.006% B, 0.042% P, and 0.5% Ti had highly ductile cup-cone fractures (Fig. 13).

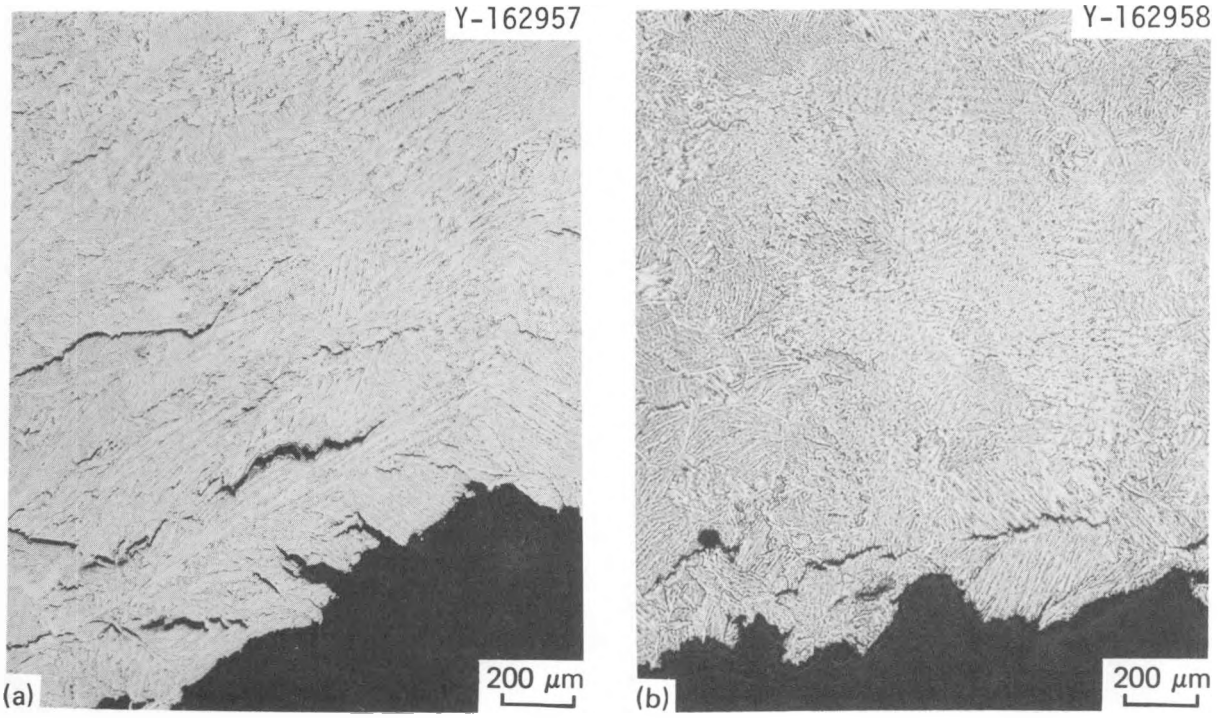


Fig. 8. Intersubstructural cracks in fractures of commercial type 308 stainless steel. (a) As-received. (b) Remelted.

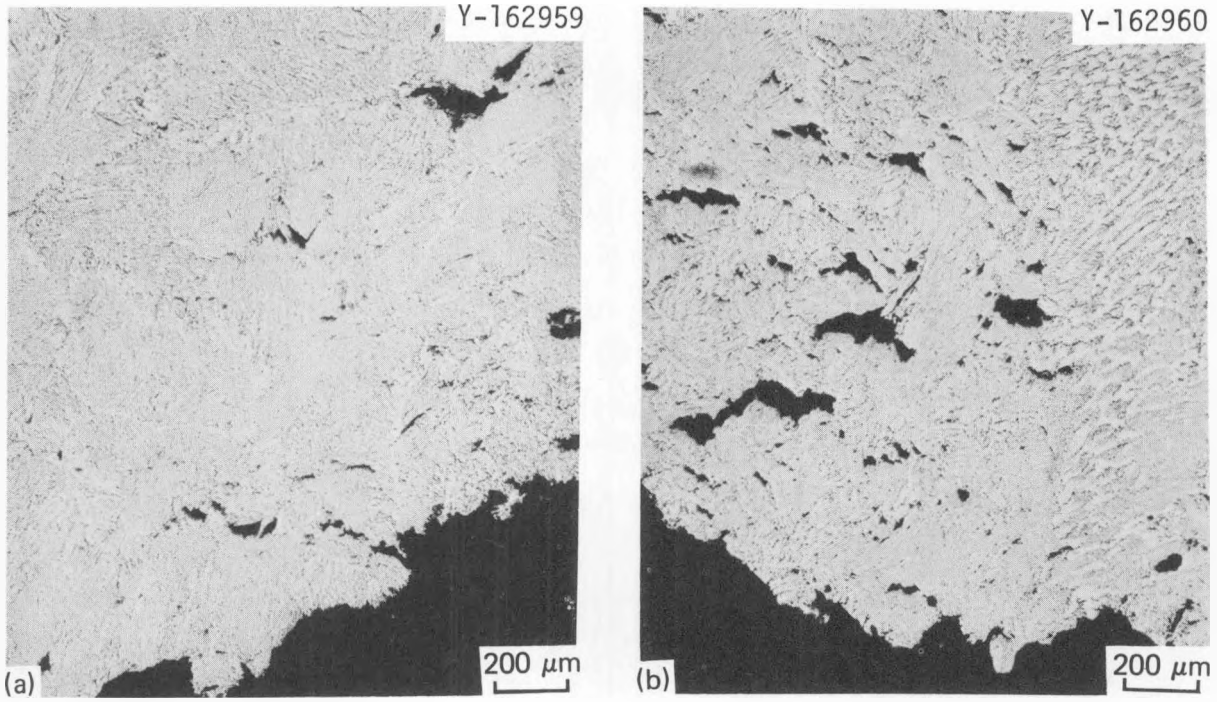


Fig. 9. Difference in fracture morphology of type 308 stainless steel. (a) With 0% Si additions. (b) With 0.6% Si additions.

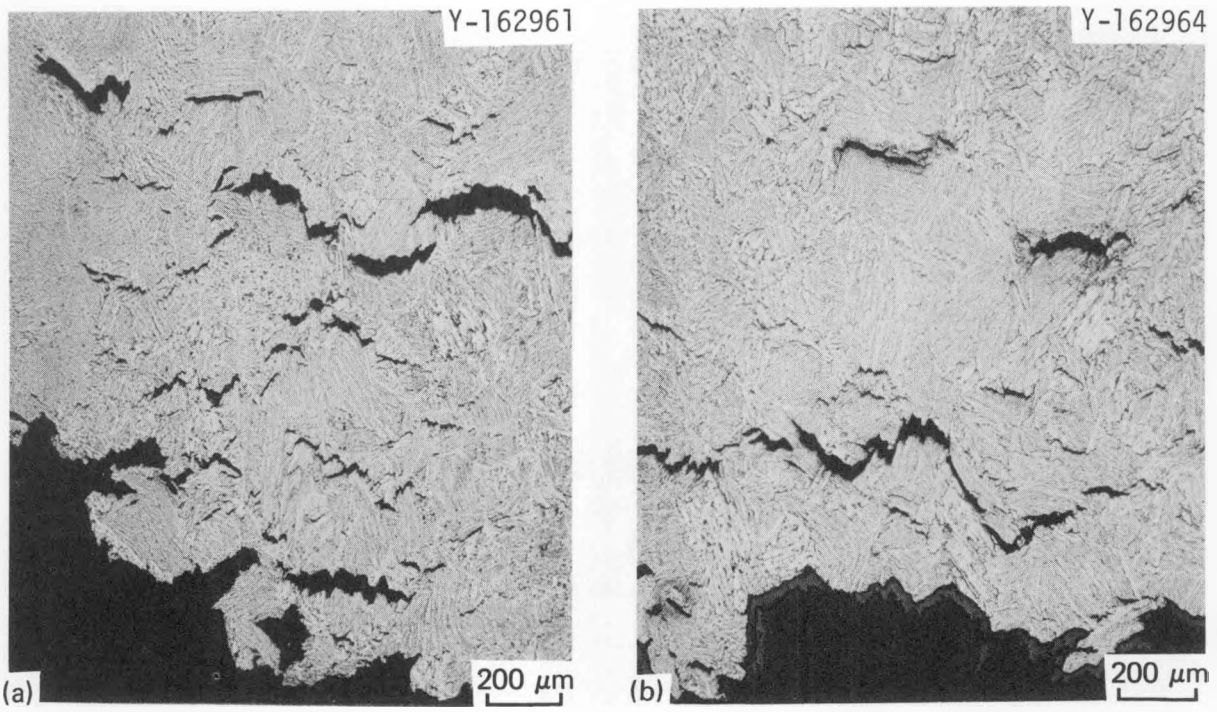


Fig. 10. Fracture morphologies of type 308 stainless steel. (a) With 0.003% B. (b) With 0.045% P.

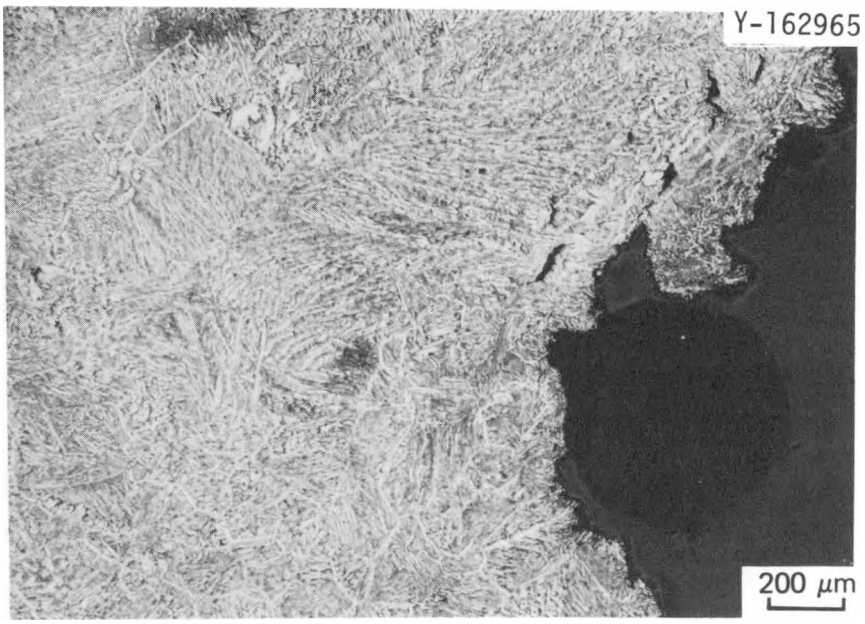


Fig. 11. Fracture morphology of type 308 stainless steel with 0.003% B and 0.051% P.

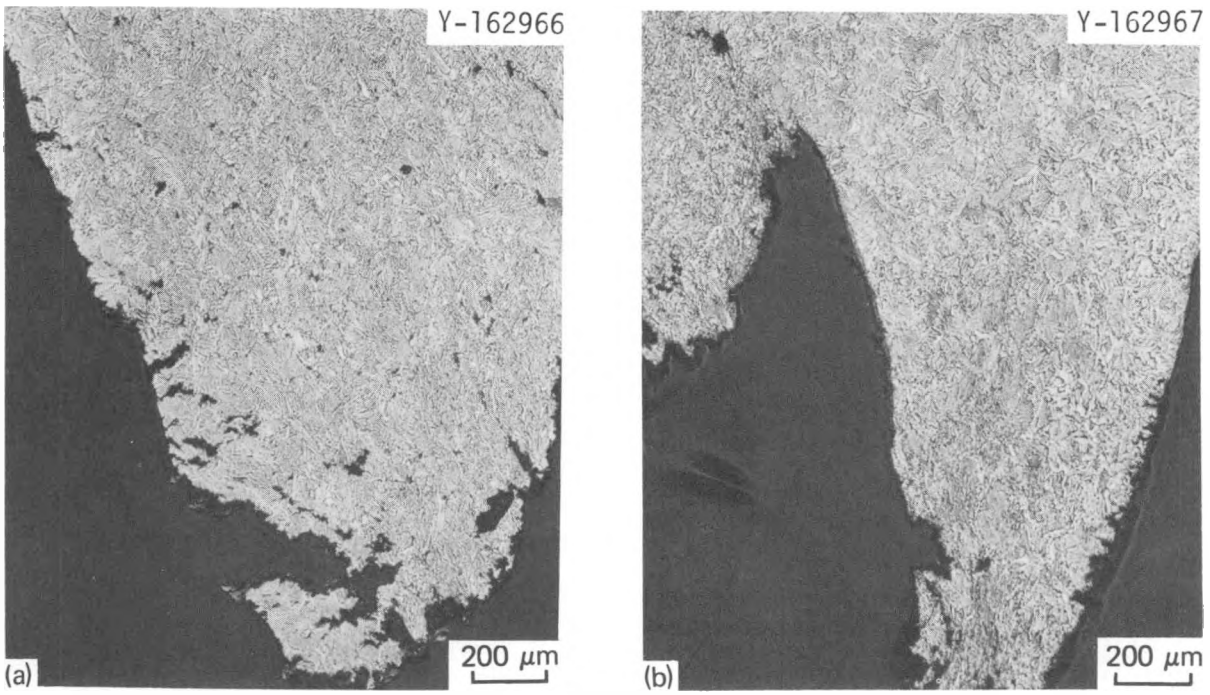


Fig. 12. Fracture morphologies of type 308 stainless steel. (a) With 0.5% Ti. (b) With 0.9% Ti.

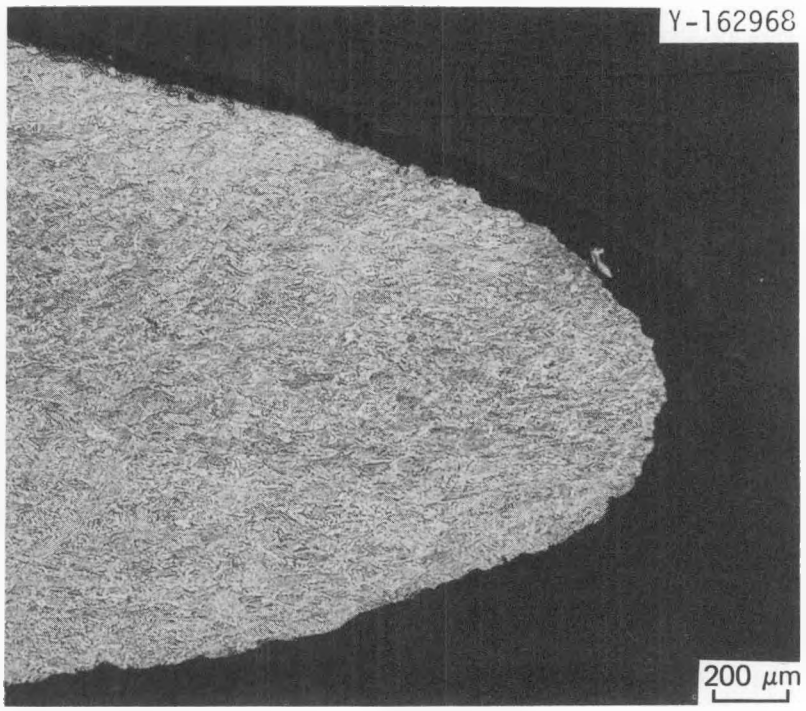


Fig. 13. Fracture morphology of type 308 stainless steel with 0.006% B, 0.041% P, and 0.5% Ti.

Close examination of the failed specimens revealed an apparent correlation between the failure mechanism and the substructure. For the specimens that failed with the least ductility and contained cracks in the specimen gage length, the cracks usually occurred within the narrow light-etching regions that surround the regions containing the lath ferrite (Fig. 14). These cracks were often at the boundaries between the austenite and the lath regions [Fig. 14(a)]. The alloys that contained only titanium had a similar δ-ferrite morphology. However, the structure is finer and no such cracks formed [Fig. 14(b)]. The width of the light-etching austenite that surrounds the lath regions in Fig. 14(b) is also narrower than it is for the alloy with cracks shown in Fig. 14(a).

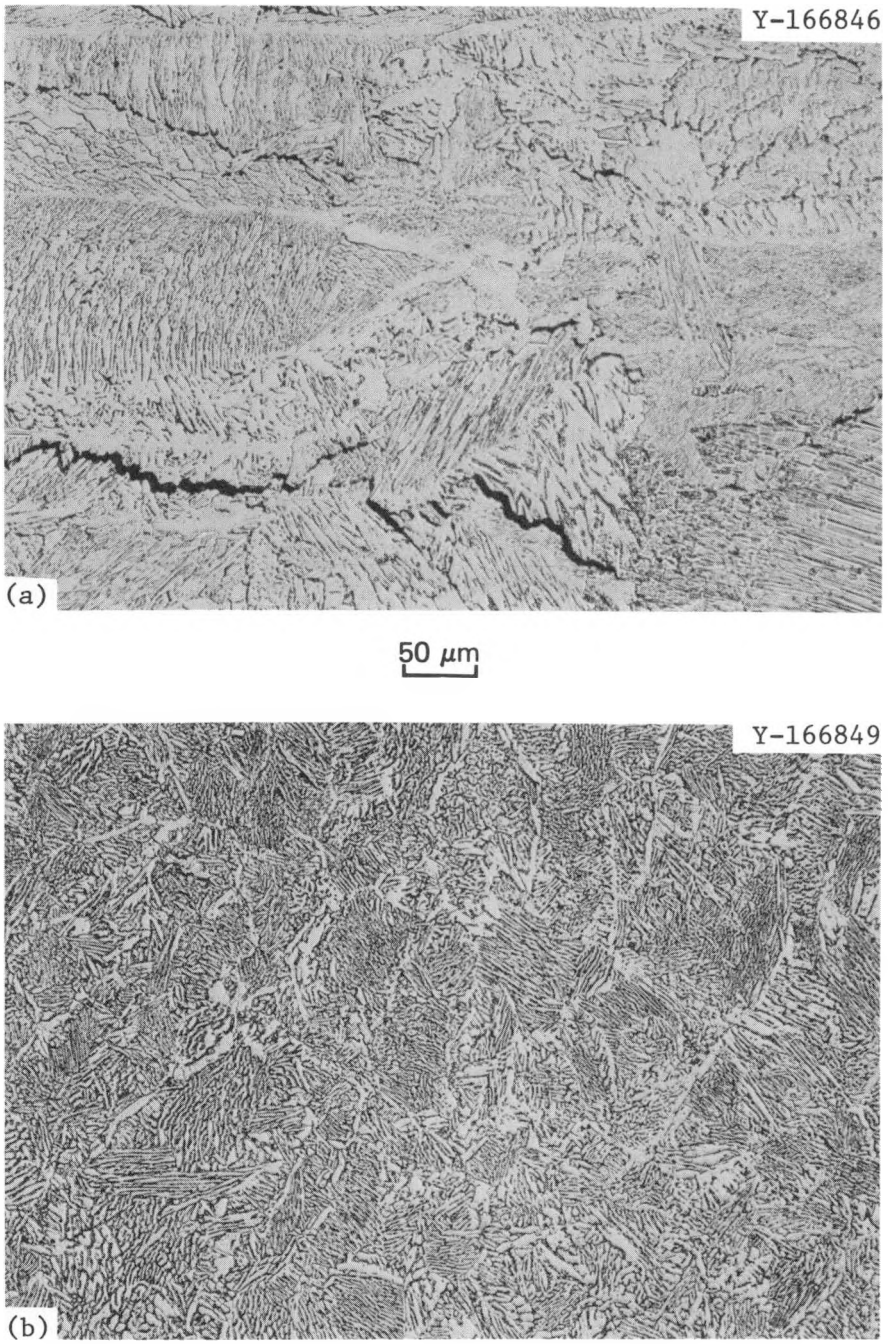


Fig. 14. High magnification of welds showing the difference in microstructure in specimen gage sections that (a) develop cracks (commercial weld) and (b) that do not (0.0006% B, 0.041% P, and 0.5% Ti).

## Type 316 Stainless Steel

Fewer type 316 stainless steel heats than type 308 stainless steel heats were studied. The effect of titanium was determined from heats for which we attempted to obtain approximately 0.3, 0.5, and 1.0% Ti. For the latter two heats, less than the desired titanium concentration was obtained (Table 2); the measured titanium concentrations were 0.29, 0.36, and 0.83%.

An increase in titanium from 0.29 to 0.36% led to a large increase in rupture strength (Fig. 15). The rupture strength for the alloy with the most titanium (0.83%) fell below that for the 0.29% Ti alloy. Thus, a peak in strength occurs again with titanium concentration. All three titanium alloys were stronger than the commercial alloy studied.

In addition to improving the strength, titanium also improved ductility. The alloy with the intermediate titanium concentration was both the strongest and the most ductile. The low-titanium alloy had the lowest ductility. Again, all three titanium alloys had better ductility than the commercial alloy.

The alloy with approximately 0.006% B and 0.042% P was not weldable because of hot cracking. However, an alloy with approximately 0.37% Ti, 0.006% B, and 0.045% P was weldable. For the long-time creep tests, the welds from this alloy showed strength and ductility comparable to or better than that of the 0.36% Ti alloy. Thus, as with the type 308 stainless steel weld metal, a combination of titanium, boron, and phosphorus in type 316 stainlesss steel also led to weld metal with superior strength and ductility (at long rupture times).

Visual observations on fractured specimens reflected the ductility measurements. The fractures on specimens from welds made with the commercial filler metal showed little or no necking; only the specimens subjected to short-time tests displayed necks. The results were similar for the welds with 0.29% Ti. The specimens with 0.37% Ti showed considerably more necking, and a decrease in neck formation occurred with decreasing stress. The welds with 0.83% Ti displayed decreasing amounts of necking with decreasing stress. Finally, the welds with 0.006% B, 0.045% P, and 0.37% Ti showed the formation of a ductile cup-cone type of fracture for all the tests.

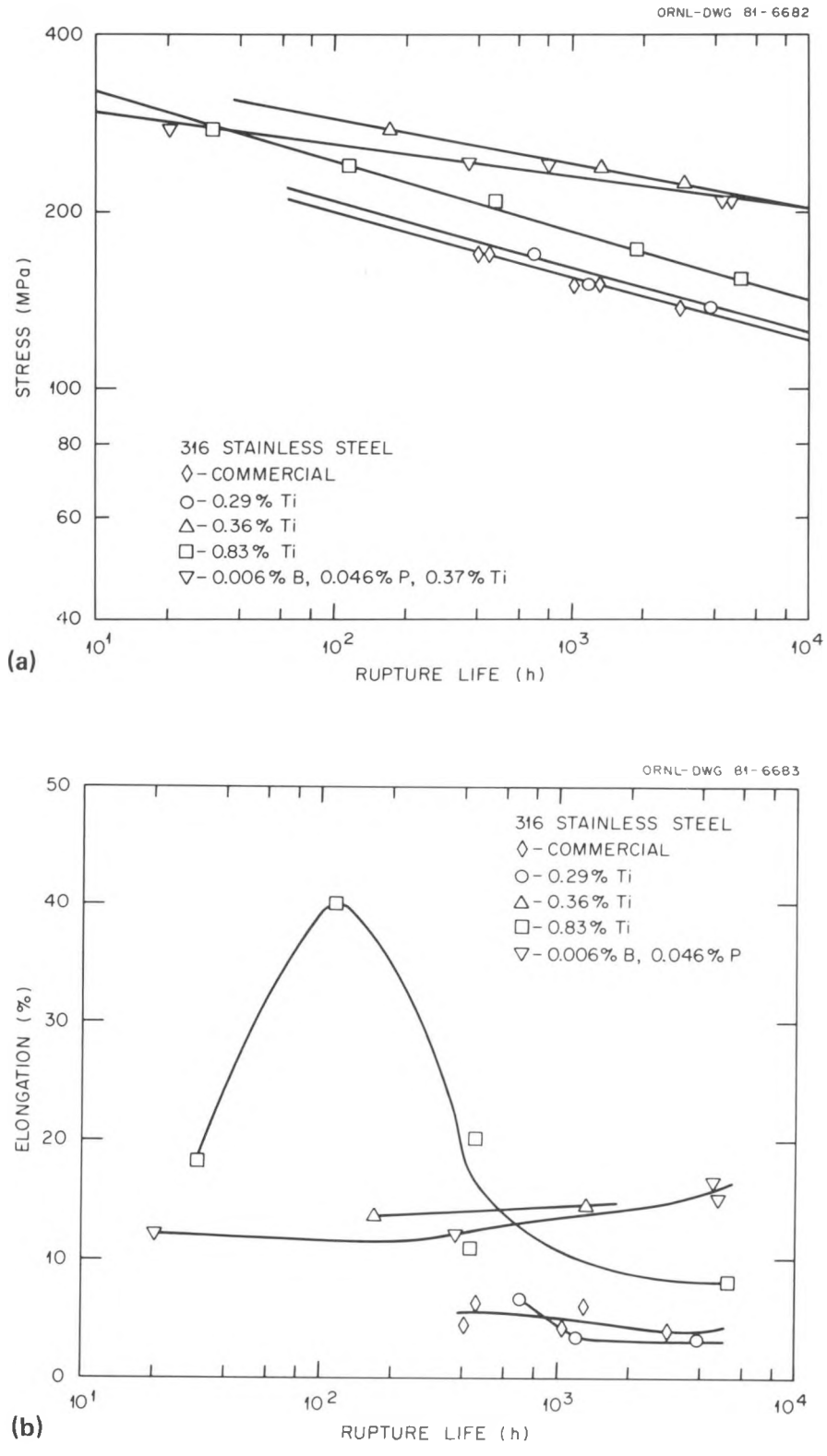


Fig. 15. Type 316 stainless steel welds deposited with commercial and experimental filler wires. (a) Stress-rupture curves. (b) Total elongation plotted against rupture life.

The overall ferrite content for the type 316 stainless steel was less than that for the type 308 stainless steel (Table 5). Again, the titanium additions increased the ferrite number well above that for alloys without titanium, and the addition of boron and phosphorus to the 0.4% Ti alloy caused a decrease in ferrite number. During exposure at 649°C in a creep test, the ferrite number decreased to zero after about 500 h.

Because of the smaller amount of δ-ferrite present in these welds, the microstructures were somewhat different from those for the type 308 stainless steel welds (Figs. 16–20). The addition of titanium again appeared to lead to a finer substructure.

Metallographic examination indicated that the commercial alloy showed considerable intersubstructural crack formation all along the specimen gage section (Fig. 21), with no necking prior to failure. The specimens with 0.29% Ti showed a small amount of neck formation. However, a considerable number of cracks occurred along the specimen gage length. The

Table 5. Ferrite number for type 316 stainless steel experimental welds

| Weld | Average ferrrite number, as welded[a] |
|---|---|
| Commercial (V-1) | 2.8 |
| Commercial (V-2) | 3.1 |
| 0.006% B, 0.042% P (V-116) | 2.0 |
| 0.006% B, 0.042% P (V-117) | 1.7 |
| 0.29% Ti (V-44) | 1.4 |
| 0.36% Ti (V-123) | 5.5 |
| 0.36% Ti (V-124) | 6.1 |
| 0.83% Ti (V-126) | 8.0[b] |
| 0.83% Ti (V-128) | 8.0[c] |
| 0.0006% B, 0.046% P, 0.37% Ti (V-122) | 6.4[d] |
| 0.0006% B, 0.046% P, 0.37% Ti (V-129) | 6.4 |

[a]After creep test at 649°C of >500 h, the ferrite number was essentially zero.

[b]Ferrite number varied from crown to root (range: 9.6–5.6).

[c]Ferrite number varied from crown to root (range: 9.0–5.2).

[d]Ferrite number varied from crown to root (range: 7.3–4.4).

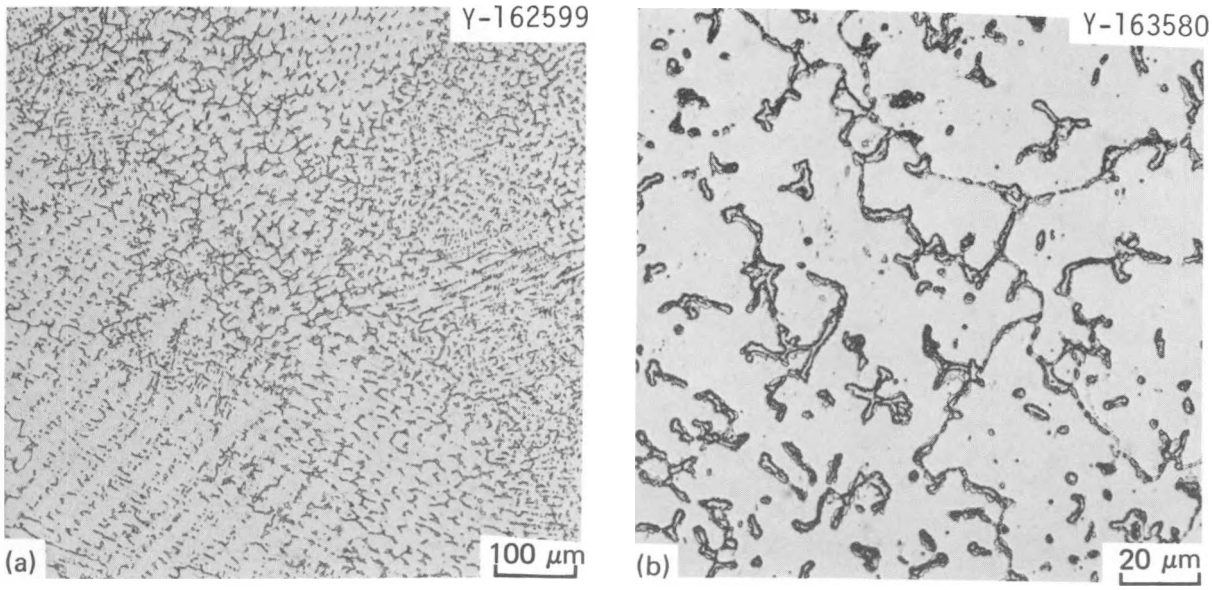


Fig. 16. Microstructure of gas tungsten arc type 316 stainless steel weld metal deposited with commercial and experimental filler wire. Etchant: aqua regia.

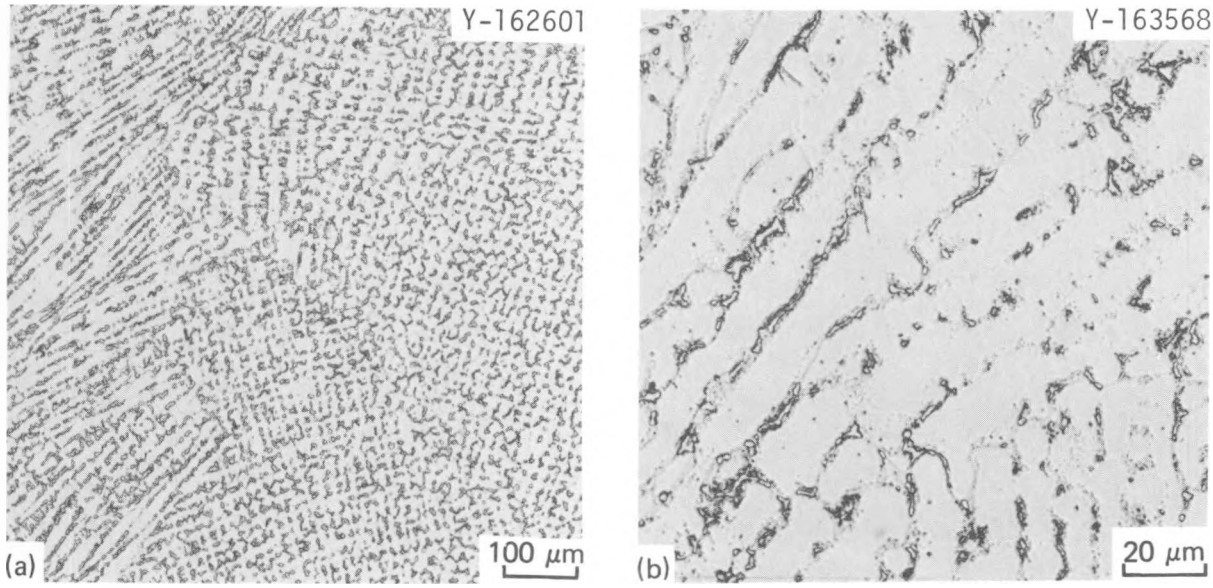


Fig. 17. Microstructure of gas tungsten arc type 316 stainless steel weld metal deposited with experimental filler wire containing 0.29% Ti. Etchant: aqua regia.

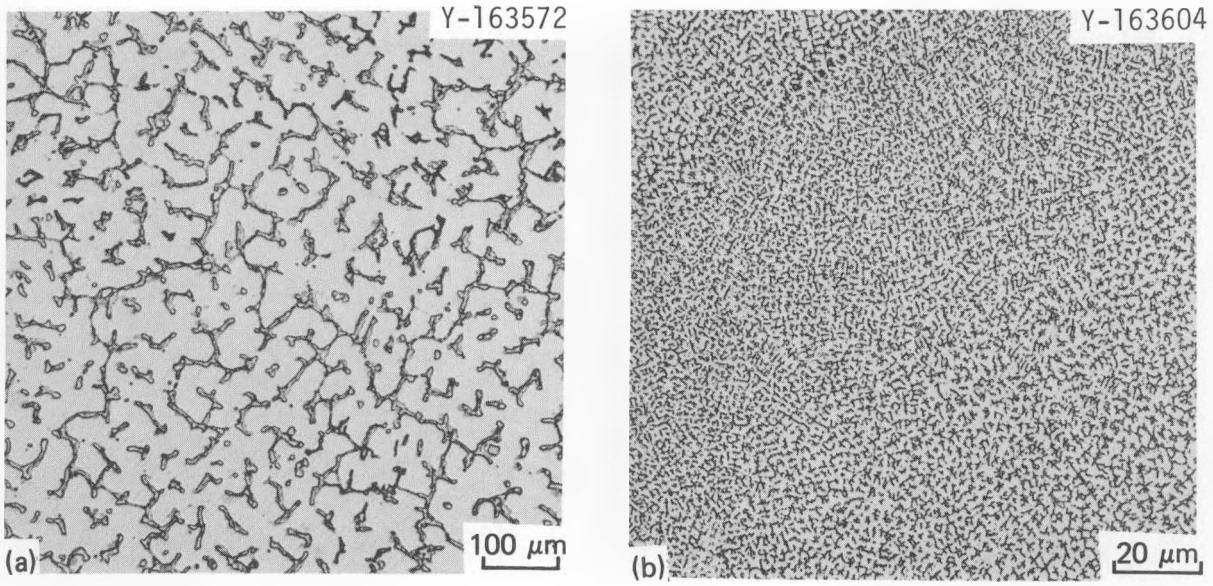


Fig. 18. Microstructure of gas tungsten arc type 316 stainless steel weld metal deposited with an experimental filler wire containing 0.36% Ti. Etchant: aqua regia.

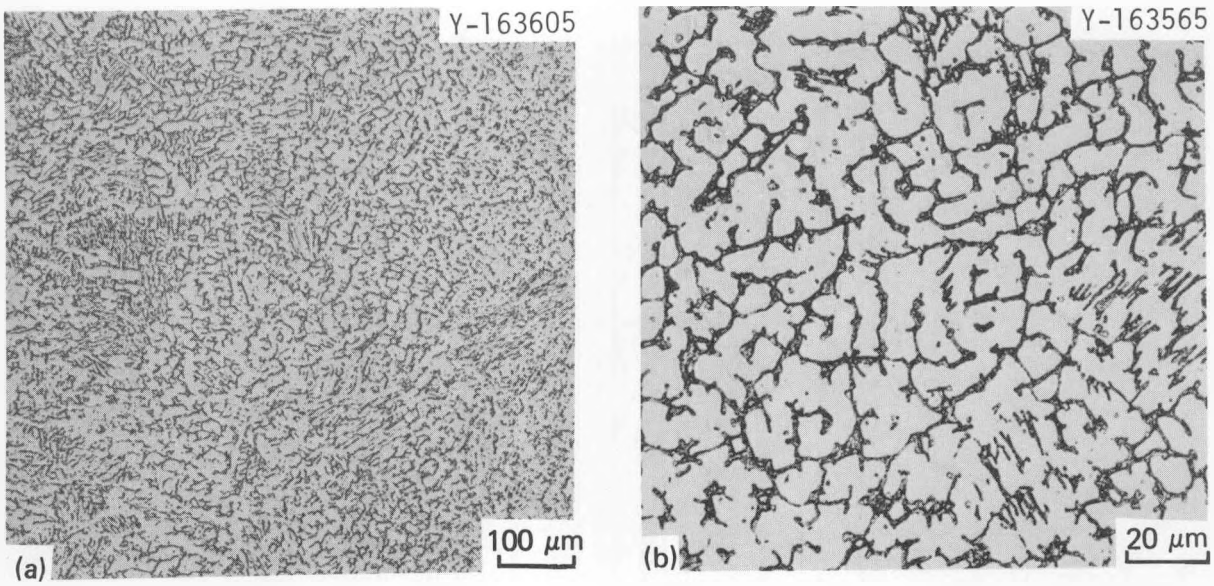


Fig. 19. Microstructure of gas tungsten arc type 316 stainless steel weld metal deposited with an experimental filler wire containing 0.83% Ti. Etchant: aqua regia.

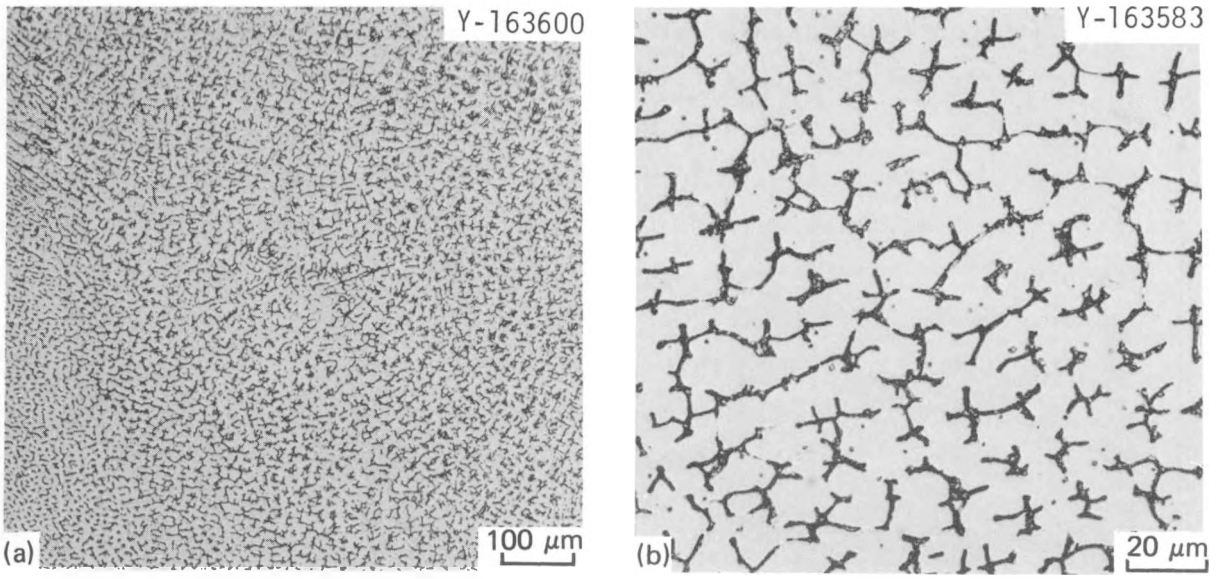


Fig. 20. Microstructure of gas tungsten arc type 316 stainless steel weld metal deposited with an experimental filler wire containing 0.006% B, 0.045% P, and 0.37% Ti. Etchant: aqua regia.

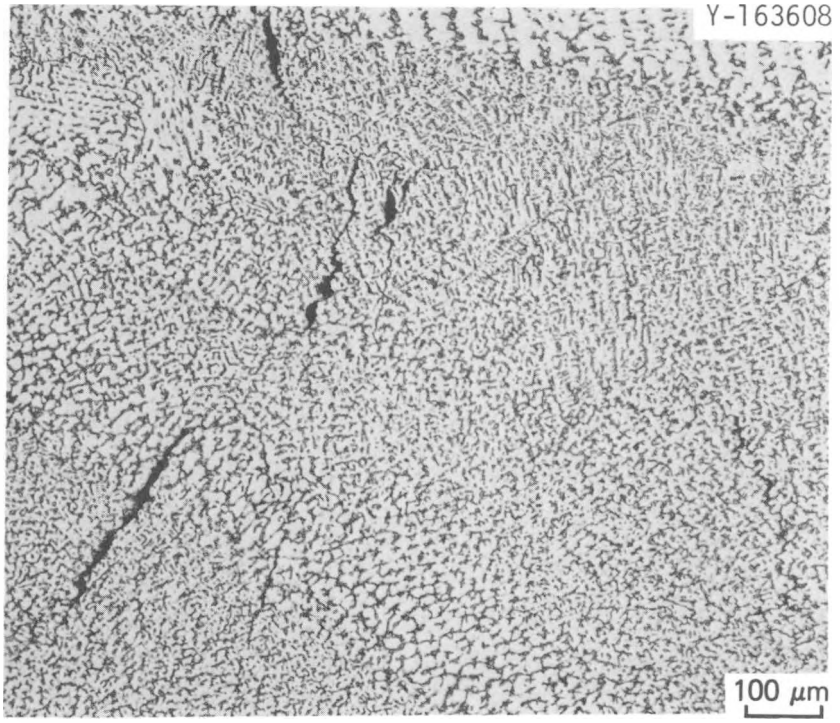


Fig. 21. Cracks in gage length of a gas tungsten arc type 316 stainless steel weld metal specimen from a weld deposited with a commercial filler wire.

specimens from the 0.36% Ti weld showed somewhat more necking. In this case holes formed very near the fracture surface. The specimens from the weld with the highest titanium content had very flat fractures. Intersubstructural cracks again formed along the specimen gage length. Finally, the specimens from the weld that contained boron, phosphorus, and titanium fractured after considerable necking — a highly ductile cup-cone type of fracture. Only a few holes, which are indicative of a highly ductile fracture, formed near the fracture surface.

If we attempt to relate the fracture modes to the weld-metal microstructures (Figs. 16–20), several interesting observations follow. The welds with superior strength and ductility were those with an intermediate ferrite content (ferrite numbers of 5.5 to 6.5, Table 5). The specimens from welds with low ferrite content (ferrite numbers of 1 to 3.5) and high ferrite content (ferrite numbers of 8) were weaker and developed intersubstructural cracks. The welds with the intermediate ferrite content (Figs. 16 and 18) had a relatively fine microstructure with the δ-ferrite much more interconnected than for the low-ferrite welds (Figs. 14 and 15) but not as interconnected as it was for the high-ferrite 0.83% Ti alloy (Fig. 17). In none of the alloys that contain titanium is there an indication of a precipitate in the light-etching austenite (Figs. 17–20).

## 16-8-2 Weld Metal

We attempted to prepare 16-8-2 filler-metal alloys with 0.5 and 1.0% Ti; an alloy with 0.006% B and 0.042% P; and one with 0.006% B, 0.042% P, and 0.5% Ti. Again, the actual chemical compositions did not always meet the intended composition (0.38% Ti instead of 0.5%; 0.79% Ti instead of 1.0%; ~0.003% B in the boron-phosphorus alloy instead of 0.006%; and 0.004% B, 0.036% P, and 0.39% Ti in the composition aimed for 0.006% B, 0.042% P, and 0.5% Ti alloy). The creep-rupture results showed considerably more scatter than observed in the types 308 and 316 stainless steel filler metals.

Figure 22 shows creep-rupture results for the experimental titanium heats and data from welds made with a commercial heat (we obtained data from welds made from nine different commercial heats of filler wire; the data shown are from the strongest of those heats). The data from different

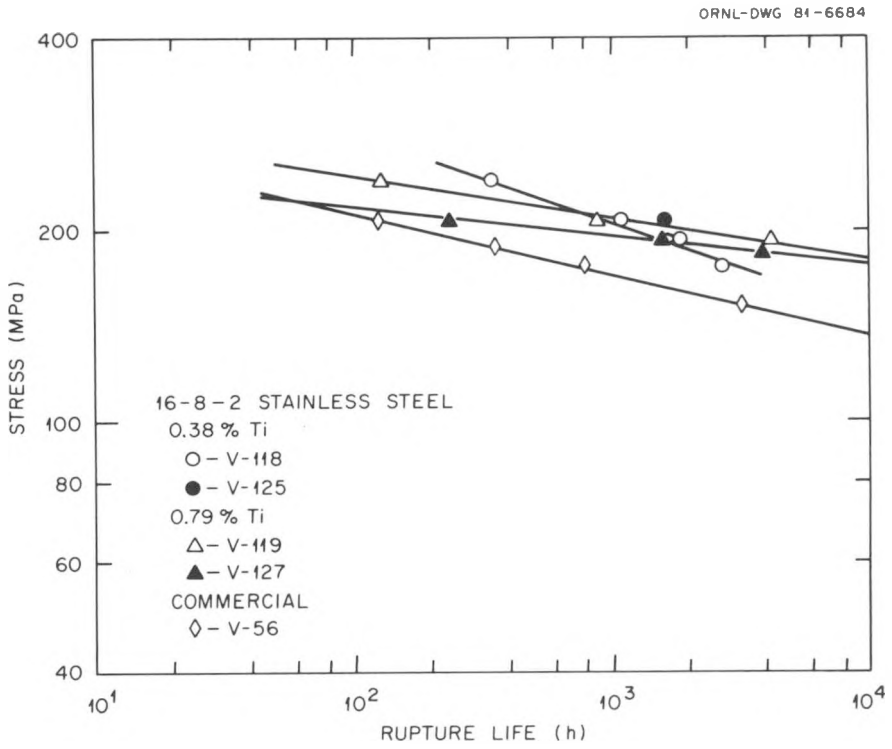


Fig. 22. Stress-rupture curves at 649°C for gas tungsten arc 16-8-2 welds deposited with commercial and experimental filler wire.

welds made from the same heat of wire for the 0.79% Ti alloy showed considerable variation, although the curves appear to converge at long rupture times. The stress-rupture curve for the 0.38% Ti weld lies above the 0.79% Ti curve at high stresses and below it for low stresses. Thus, the addition of titanium gives a significantly stronger material than welds made with the commercial wire. If there is a strength peak with titanium concentration (as was true for types 308 and 316 stainless steel) it must be above 0.8% Ti.

In Fig. 23 the data for the heat with boron and phosphorus and with boron, phosphorus, and titanium are compared with one weld with about 0.38% Ti and the commercial heat. The strength of the heat with the boron and phosphorus additions was similar to that of the 0.38% Ti alloy. The creep-rupture strength for the weld that contained boron, phosphorus, and titanium was much greater than that for the other alloys.

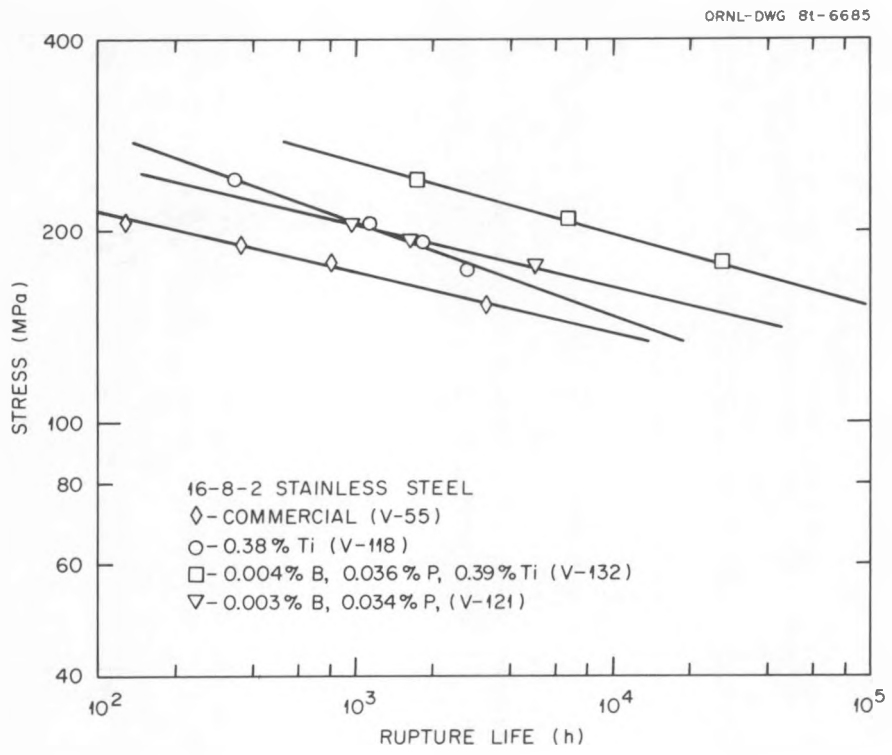


Fig. 23. Stress-rupture curves at 649°C for gas tungsten arc type 16-8-2 welds deposited with commercial and experimental filler wire.

The total elongation of the various welds showed relatively little difference for the various heats for creep-rupture lifetimes between several hundred and several thousand hours (Fig. 24). The heat with boron and phosphorus had the greatest elongation in this range, and the 0.38% Ti alloy had the least.

Visual examination of fractured specimens indicated that the commercial alloys had quite ductile fractures with some neck formation. The amount of necking generally decreased with decreasing stress (increased rupture life). The considerably less ductile alloy with 0.38% Ti fractured with little neck formation. The high-titanium alloy displayed more ductility, although the fractures became flatter (less necking) with decreasing stress. The alloy with boron and phosphorus additions behaved like the high-titanium alloy, with the amount of necking decreasing (flatter fractures) with decreasing stress. Finally, the alloy to which boron, phosphorus, and titanium were added was quite ductile, even the specimen that failed after 26,000 h.

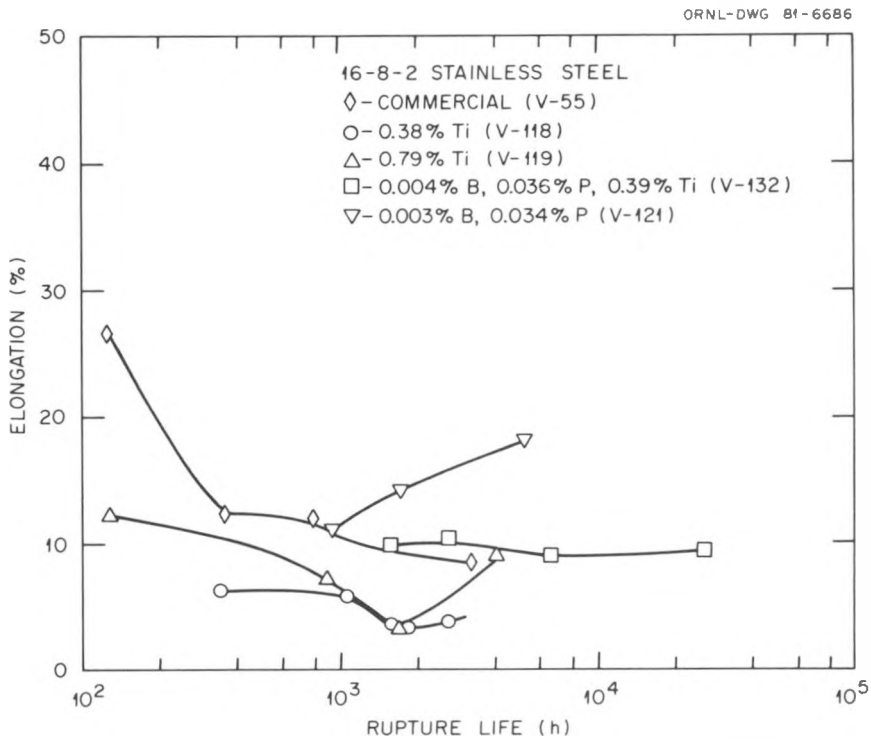


Fig. 24. Total elongation plotted against rupture life at 649°C for gas tungsten arc type 16-8-2 welds deposited with commercial and experimental filler wire.

Ferrite content again reflected the effect of titanium: an increase in titanium increased the ferrite number (Table 6). The commercial alloys had the lowest ferrite numbers, the 0.79% Ti alloy the highest.

Metallographic observations on the specimens are in general agreement with the ductility measurements and the visual observations on the fractures. Reduced ductility coincided with an increase in the number of intersubstructural cracks in the specimen gage length, as was observed for the types 308 and 316 stainless steel weld metals.

Although microstructures differ from one weld to another, correlating these differences with the properties is difficult. Futhermore, every specimen has a range of microstructures on a given longitudinal section. The microstructures of the commercial alloys were quite coarse (Fig. 25). Additions of titanium led to a much finer microstructure (Fig. 26). The microstructure of the weld with boron and phosphorus additions was quite coarse (Fig. 27). A still different structure was present for the alloy

Table 6. Ferrite number for 16-8-2 stainless steel experimental welds

| Weld | Average ferrrite number, as welded |
|---|---|
| Commercial (V-55) | 3.2 |
| Commercial (V-56) | 2.9 |
| 0.003% B, 0.034% P (V-121) | 4.0 |
| 0.38% Ti (V-118) | 6.3 |
| 0.38% Ti (V-125) | 4.9 |
| 0.79% Ti (V-119) | 10.1[a] |
| 0.79% Ti (V-127) | 13.6[b] |
| 0.004% B, 0.036% P, 0.4% Ti (V-132) | 6.2 |

[a]Ferrite numbers varied greatly from crown to root (range: 18.0–4.2).

[b]Ferrite numbers varied greatly from crown to root (range: 18.3–5.1).

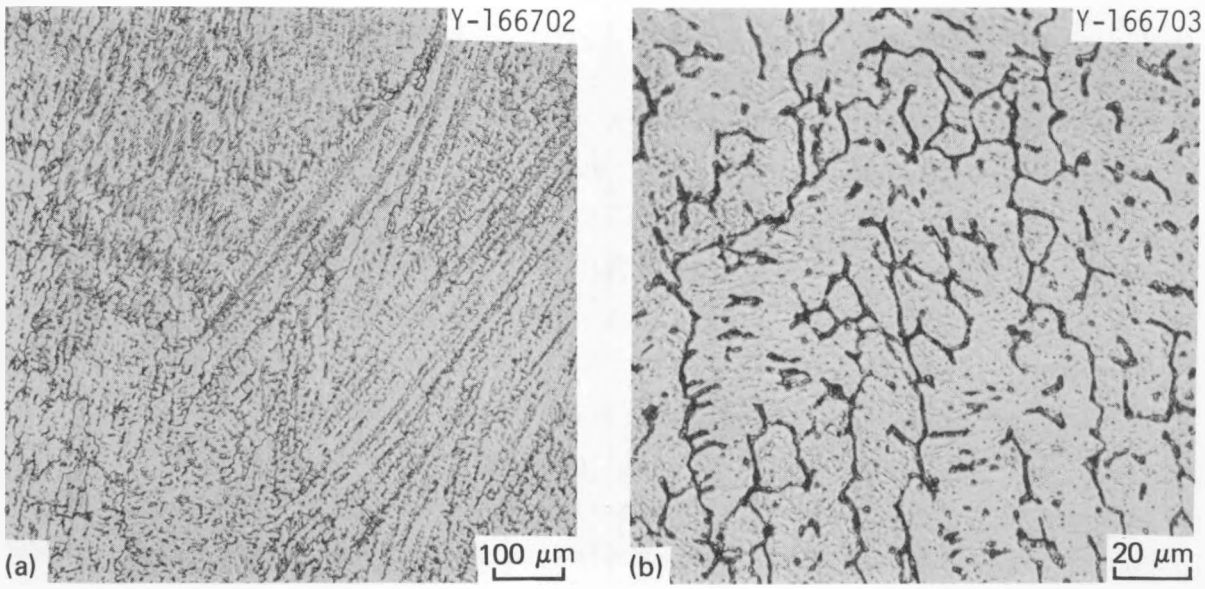


Fig. 25. Microstructure of gas tungsten arc type 16-8-2 weld metal deposited with commercial filler wire. Etchant: aqua regia.

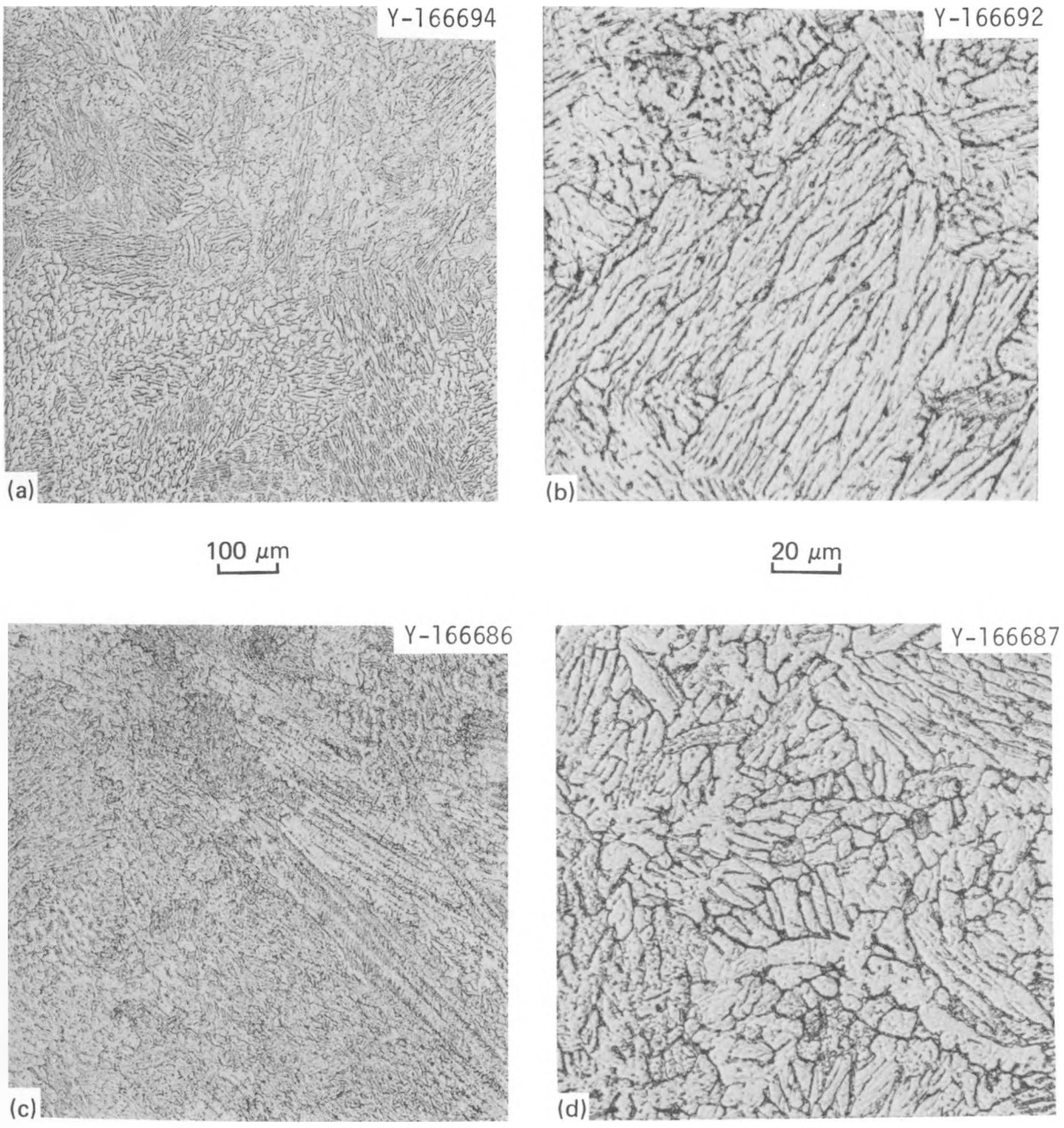


Fig. 26. Microstructure of gas tungsten arc type 16-8-2 weld metal deposited with an experimental filler wire. (a) and (b) 0.38% Ti. (c) and (d) 0.79% Ti. Etchant: aqua regia.

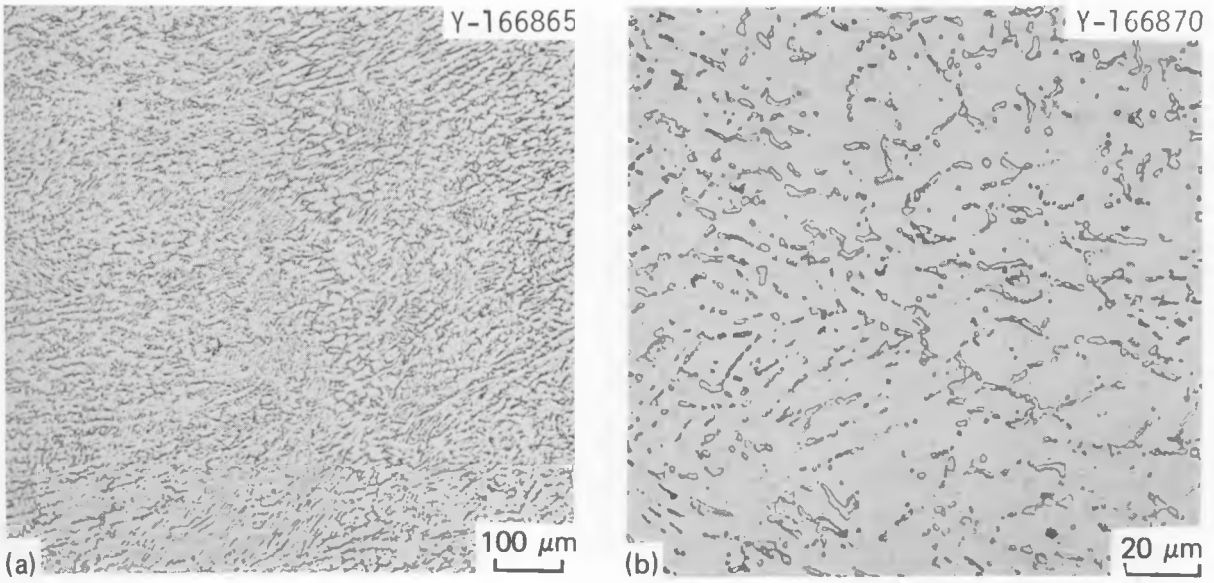


Fig. 27. Microstructure of gas tungsten arc 16-8-2 weld metal deposited with an experimental filler wire with 0.003% B and 0.034% P. Etchant: aqua regia.

with titanium, boron, and phosphorus additions (Fig. 28). However, we again emphasize that there was a range of microstructures for any given specimen, depending on the weld pass and the position in the pass relative to adjacent passes.

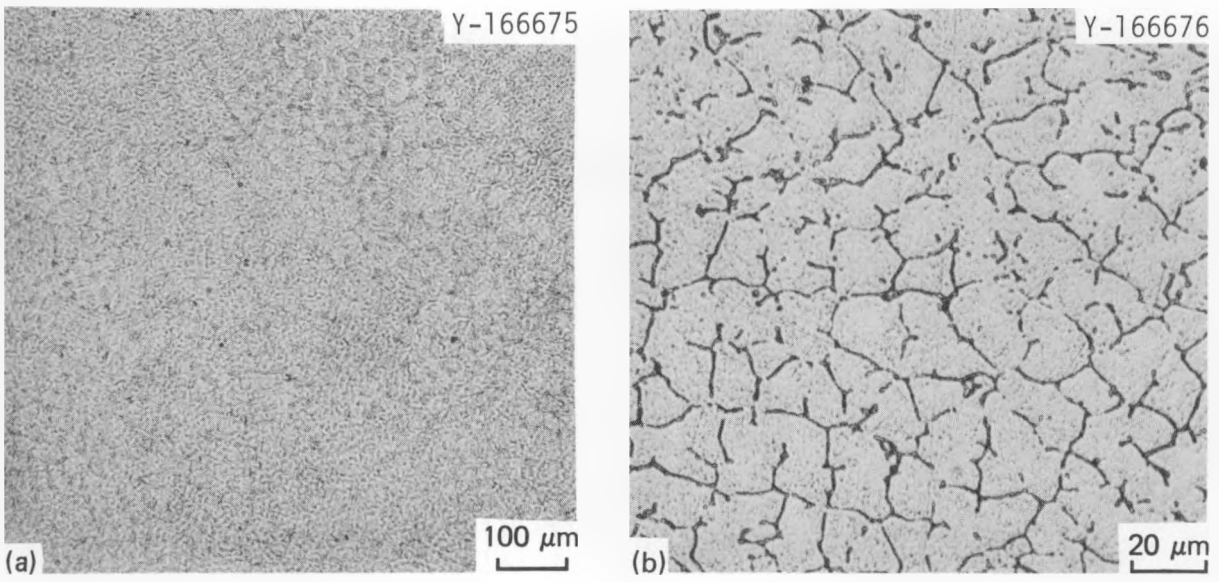


Fig. 28. Microstructures of gas tungsten arc type 16-8-2 weld metal deposited with an experimental filler wire with 0.006% B, 0.042% P, and 0.38% Ti added. Etchant: aqua regia.

# DISCUSSION

The results of these studies demonstrated an effect of titanium, phosphorus, and boron on the strength and ductility of the GTA welds deposited with the austenitic stainless steel filler metals of types 308, 316, and 16-8-2. For all three materials a combination of the three elements caused an increase in strength and ductility over the welds deposited with commercial filler metals and over those of the respective alloys with either titanium, phosphorus, or boron additions singularly or a combination of phosphorus and boron. In addition to the strength differences, the addition of titanium, phosphorus, and boron individually and in combination caused microstructural differences. We discuss first the microstructural changes caused by the addition of these three elements and then their effect on the creep strength.

Several investigators have attempted to classify the microstructures of austenitic stainless steel welds on the basis of δ-ferrite morphologies.[6–9] There are basically two types of microstructures, termed "vermicular"[6–9] and "lathy"[8] or "acicular."[9] These microstructures have been observed in the current study (Fig. 29). The type of microstructure observed depends on the ferrite content: the vermicular structure occurs for a low-volume fraction of ferrite ($\lesssim$6%) and acicular at higher ferrite contents ($\gtrsim$12%). These two microstructures have been further classified into three categories by Suutala, Takalo, and Moisio[8] and into four categories by David.[9] David showed that a more complicated vermicular structure is often observed, which he labeled "lacy." He also identified a "globular" structure, which appears to evolve from the acicular structure when heated by subsequent weld passes.[9]

As pointed out by David,[9] the ferrite content, as well as the microstructure, can vary across a given weld. These variations are the result of different cooling rates, weld metal composition differences due to base metal dilution, and dissolution of ferrite resulting from thermal cycles during subsequent weld passes. Such variations were noted in the welds made for this study. However, the microstructure generally showed little variation across the region in the center of the weld where the

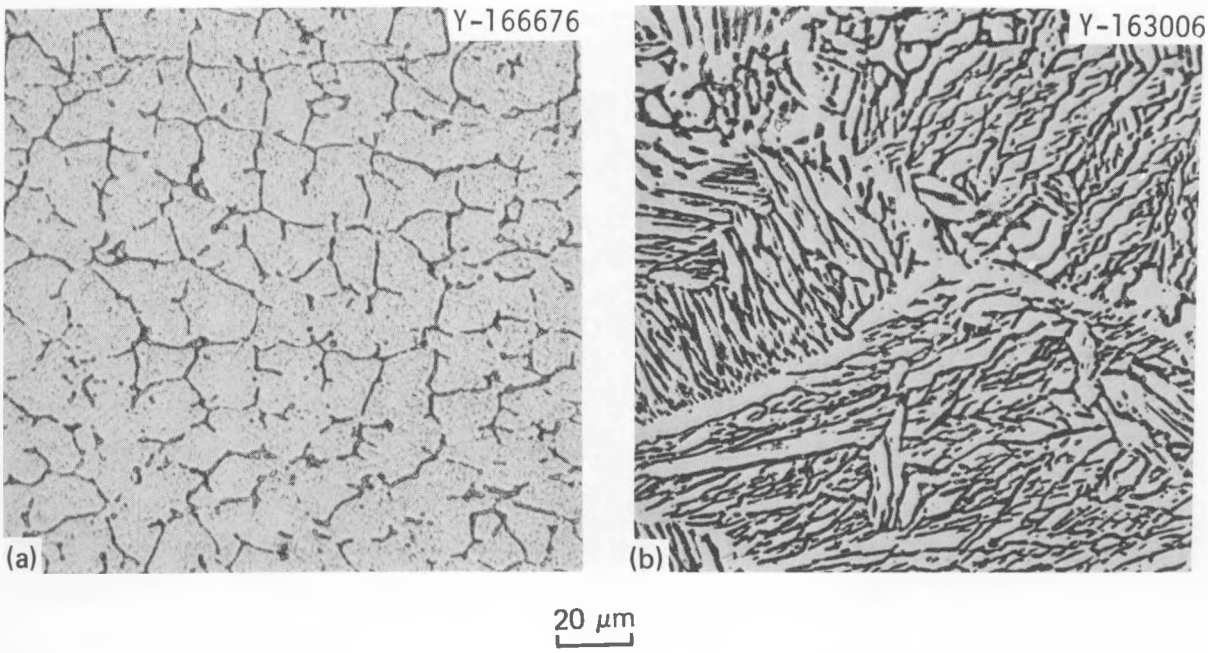


Fig. 29. Examples of different types of weld-metal microstructures observed: (a) "Vermicular" structure of experimental type 16-8-2 weld with boron and phosphorus additions. (b) "Lathy" or "acicular" structure of type 308 stainless steel weld with boron and phosphorus additions. Etchant: aqua regia.

3.2-mm-diam test specimens were taken (the 16-8-2 welds showed the most variation in microstructure and the largest variation in ferrite number across the weld). The microstructures presented were representative of the position of the tensile specimens.

From an examination of the microstructures of the types 308 stainless steel (Figs. 5–7) and 316 stainless steel (Figs. 16–20) weld metals, it appeared that ferrite morphology must play a relatively minor role in the change in strength and ductility that accompanies the change in chemical composition. The type 308 stainless steel weld metals were basically acicular and the type 316 stainless steel basically vermicular regardless of the composition. Thus, the change in strength caused by the addition of titanium, boron, and phosphorus is caused by something other than a microstructural change. In the case of the 16-8-2 weld metal, the large microstructural variability makes it much more difficult to make a statement concerning a relationship between ferrite morphology and composition.

Nevertheless, for this discussion we assumed that the change in strength and ductility accompanying the boron, phosphorus, and titanium additions was caused by something other than the change in ferrite microstructure.

Delta-ferrite content is known to affect the strength of austenitic stainless steel base metals.[10] Titanium,[11–13] phosphorus,[14–17] and boron[18–20] additions to these base metals are also known to affect the creep strength and ductility. These strength changes occur in the base metals that contain essentially no δ-ferrite. When an austenitic stainless steel weld metal is tested in creep (or thermally aged) at 500 to 900°C, the δ-ferrite can transform to the hard, brittle intermetallic phases, such as the sigma phase.[21] Fracture at the intermetallic-austenite boundary can lead to a significant reduction in ductility.[5,22] Because the strength and ductility both increased with some of the changes in chemical composition that also led to higher δ-ferrite contents and presumably larger amounts of sigma, the processes are undoubtedly quite complicated. Much more work will be required before these processes are completely understood. In this discussion we examine what is known about the effects of titanium, phosphorous, and boron on the strength of austenitic stainless steel base metals and indicate how they may affect the weld metals.

Bloom did creep-rupture studies at 700 and 815°C on type 304 stainless steel (chemical composition is similar to type 308 stainless steel) with 0.15% Ti and compared the results with type 304 stainless steel without titanium.[11] When tested in the solution-annealed condition (1 h at 1038°C), the rupture life and ductility of the titanium-modified steel were increased significantly over the values for the unmodified alloy. A ductile transgranular fracture mode was observed for the titanium-modified steel, whereas the fracture mode of the unmodified steel was intergranular and much less ductile than the modified steel. All these observations are similar to the effect of titanium noted for the weld metals.

Transmission electron microscopy studies by Bloom[11] revealed that during a creep test of the solution-annealed titanium-modified type 304 stainless steel, very fine titanium carbides precipitated on dislocations, thus locking them and increasing the strength. When aged before testing, most of the carbides precipitated on grain boundaries. In the unmodified

alloy most of the precipitation ($M_{23}C_6$) was confined to grain boundaries; the precipitation in the matrix consisted of relatively few large globular precipitates.[11]

Bloom, Leitnaker, and Stiegler[13] attributed the reduced tendency toward grain boundary cracking to the removal of surface-active elements such as sulfur and nitrogen. Titanium is known to remove these impurities from solution by forming $Ti_4C_2S_2$ and Ti(CN) (ref. 23). Bloom and coworkers concluded that the removal of these elements from the grain boundaries strengthened the boundaries and reduced grain boundary cracking.[13]

Because the weld metals of the current study were cooled quite quickly from the melt, we would expect most of the titanium to be in solution before testing. The analogus behavior of titanium in the weld metals and austenitic stainless steel base metals leads to the conclusion that the increased strength and ductility must be caused by processes similar to those that occur in the base metal.

Further evidence of a similar behavior in weld metal and base metal is obtained from the Bloom, Leitnaker, and Stiegler studies on the effect of titanium concentration on the creep-rupture properties of type 316 stainless steel.[13] Tests were made at 241 MPa and 650°C on type 316 stainless steel with 0, 0.23, 0.33, 0.46, and 0.60% Ti. In Fig. 30 these rupture life data are compared with the data from the current study on type 316 stainless steel weld metal with 0, 0.29, 0.36, and 0.83% Ti. The similarity in behavior is again obvious. Both the base metal and weld metal show peaks in rupture life at intermediate titanium concentrations. The peak for the weld metal is higher and appears to be displaced toward higher titanium concentrations.

The effect of the titanium in type 316 stainless steel base metal was again attributed to a fine precipitate in the austenite matrix[13] (there is no δ-ferrite present in the base metal). In the weld metal the δ-ferrite would be expected to be enriched in titanium, a ferrite-forming element. Thus, all the titanium added to the weld metal is not available for strengthening the austenite. This leads to displacement of the peak to higher concentrations. The titanium in the δ-ferrite and the formation of Ti(CN) and $Ti_2C_2S_4$ (ref. 13) can probably account for the relatively small effect of titanium at low concentrations.

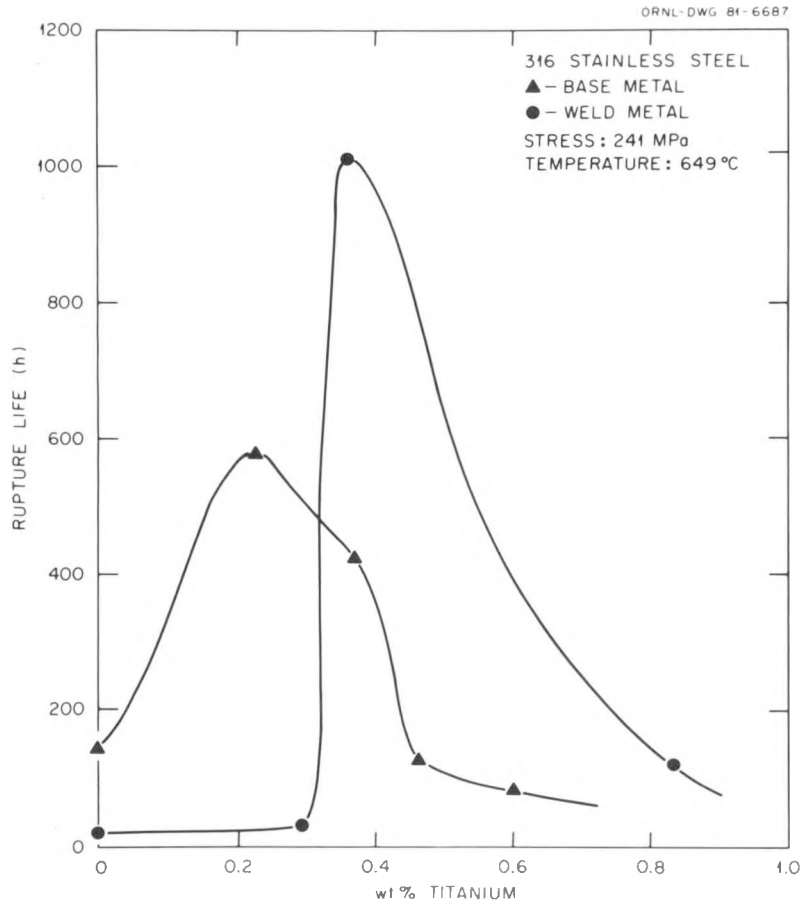


Fig. 30. The rupture life plotted against titanium concentration for type 316 stainless steel weld metal and base metal. Source of base metal results: E. E. Bloom, J. M. Leitnaker, and J. O. Stiegler, "Effect of Neutron Irradiation on the Microstructure and Properties of Titanium-Stabilized Type 316 Stainless Steels," *Nucl. Technol.* 31: 232–43 (1976).

The difference in peak height may be due to the titanium concentrations for which measurements were made. That is, the peak strength of the base metal may occur for an alloy with titanium concentrations between 0.23 and 0.33% or between 0 and 0.23% where no measurements were made. Another possibility is that the weld metal peak strength is enhanced by the δ-ferrite. However, the comparative strengths of weld metal and base metal on either side of the peaks do not support this latter hypothesis.

The similarity of the effect of titanium on base metal and weld metal appears to indicate that titanium plays a similar role in both. In addition to the beneficial role of titanium, phosphorus and boron also affected

the creep-rupture properties. Only in the type 308 stainless steel weld metal did we attempt to determine the effect of phosphorus and boron individually and in combination with one another (Fig. 3), and, finally, the two in combination with titanium (Fig. 4). We observed a minor effect of phosphorus on strength for the 0.049% P alloy [Fig. 3(a)]. A somewhat larger effect was observed for the 0.003 and 0.013% B alloys. The combination of 0.051% P and 0.007% B had an effect on strength considerably greater than either element individually. The effects of the two species appear to be additive relative to the commercial filler metal (Fig. 3). Furthermore, at long rupture times the alloy with both elements had ductility superior to the alloys containing only one of these species.

Studies on the effect of phosphorus and boron individually on the strength and ductility of type 18-8 austenitic stainless steels have been reported.[14–19] In the case of phosphorus, the concentrations studied were generally about 10 times those used in this study. It has been shown that phosphorus can augment dispersion hardening caused by carbon.[13] Several explanations have been offered. Most generally it is concluded that phosphorus enters into the $M_{23}C_6$ in the form $M_{23}(CP)_6$ (refs. 15 and 16). It also affects the morphology of the precipitate; that is, it gives rise to a finer matrix precipitate than when phosphorus is not present.[15,16] It is also felt that it increases ductility by leading to less grain boundary precipitates.

Rowcliffe and Nicholson[17] studied the effect of phosphorus on precipitation in a low-carbon type 18-10 stainless steel with 0.3% P and found that, when these alloys were quenched from 1300°C, a variety of vacancy defects were formed. They concluded that the defects were formed as a result of an interaction between vacancies and phosphorus atoms. Eventually these vacancy defects acted as nucleation sites for $Cr_3P$ precipitates. The authors felt a similar process could be responsible for the influence of phosphorus on carbide precipitation observed in steels with higher carbon contents.

Boron has also been found to have an effect on precipitation in austenitic stainless steels. Henry and coworkers[18–20] found that the addition of boron up to 0.015% led to a marked improvement of hot strength

and room temperature ductility of 18 Cr—12 Ni—3 Mo (a composition similar to type 316 stainless steel). They concluded that the boron influenced the nucleation of the $M_{23}C_6$ and the subsequent interaction of this precipitate with dislocations.[18,19] Boron was also thought to decrease the solubility of carbon in the stainless steel.

The above discussion shows that titanium, phosphorus, and boron can individually increase the strength and ductility of austenitic stainless steels. Without further studies, it is not possible to state that the enhanced strength and ductility of the Ti-P-B alloy over the alloys with these elements added individually is more than a simple additive effect of these three elements.

The most interesting observation is that the effect of the titanium, phosphorus, and boron in the weld metal is similar to the effect in the base metal, even though the microstructures are different. If the low ductility of the commercial weld metal is caused by the weakness of the sigma-austenite interface, the increased ductility of the weld metal is due to the fact that the effect of the three elements at this interface is similar to the effect they have on the grain boundaries of the base metal. This effect occurs despite the fact that, in the case of the alloys with the titanium additions, more δ-ferrite, and thus more of the brittle sigma phase, forms. The only factor common to the base metal and weld metal appears to be the precipitates. This seems to indicate that the titanium, phosphorus, and boron play the same role on the precipitates in the sigma-austentite intersubstructural boundaries as in the grain boundaries of the base metal. It should be pointed out that the intersubstructural separations in the weld-metal alloys of low ductility occur at boundaries that are analogous to grain boundaries in a base metal (Fig. 14). This can be seen in the difference in orientation of the δ-ferrite (sigma) on opposite sides of a crack.

## SUMMARY AND CONCLUSIONS

We investigated the effect of alloying additions on the elevated-temperature strength and ductility of austenitic stainless steel weld metals. Controlled additions of Si, Ti, P, and B were made to the commercial compositions for types 308, 316, and 16-8-2 stainless steel filler

metals. These experimental filler-metal alloys were then used to make GTA welds. Creep-rupture tests at 649°C were made on specimens taken from these welds. The observations and conclusions for each of the stainless steel alloys are given below.

Nominal additions of 0.5 and 0.9% Ti increased the strength and ductility of type 308 stainless steel; the 0.5% Ti addition had the greater effect. Silicon additions to the commercial composition for type 308 stainless steel had little effect on strength and ductility. Minor additions of boron and phosphorus increased the strength slightly, but additions of the combination (0.003% B and 0.051% P) gave essentially an additive effect. This combination of alloying elements did not give effects as great as the nominal 0.5 and 1.0% Ti additions. Finally, the addition of 0.041% P, 0.006% B, and 0.5% Ti to the type 308 stainless steel composition produced an alloy with the greatest strength and ductility.

Similar types of alloying additions were made to the commercial composition for type 316 stainless steel. Again, a combination of approximately 0.042% P, 0.006% B, and 0.5% Ti gave an alloy with the best strength and ductility. However, in this case the superiority of this alloy over that with only the 0.5% Ti addition had to be inferred from extrapolations to low stresses (long rupture lifetimes). For short creep-rupture times the 0.5% Ti alloy clearly had better properties.

Our creep-rupture studies on the 16-8-2 weld metals gave results that were not as easily interpreted as were those for types 308 and 316 stainless steel. Extrapolation to low stresses indicated that the 1.0% Ti alloy would have a strength advantage over that with 0.5% Ti. The alloy with approximately 0.045% P and 0.006% B had a strength and ductility similar to that of the 1.0% Ti alloy. All alloys were significantly better than the commercial alloy.

The effect of the titanium, phosphorus, and boron on the stress-rupture properties of the weld metal were compared with their effect in similar austenitic stainless steel base metal. Similar effects were observed, indicating that the processes that occur in the two types of microstructure are similar. This similarity occurred despite the fact that the weld metal microstructures contained nearly 20% δ-ferrite.

ACKNOWLEDGMENTS

Special thanks are due to several people. E. Bolling carried out the experimental work. C. W. Houck did the metallography. The manuscript was reviewed by S. A. David and R. W. Swindeman. Irene Brogden edited the manuscript, and A. J. Carter prepared the final copy.

REFERENCES

1. N. C. Binkley, G. M. Goodwin, and D. G. Harman, "Effects of Electrode Coverings on Elevated-Temperature Properties of Austenitic Stainless Steel Weld Metal," *Weld. J. (Miami)* 52(7): 306-s–11-s (1973).
2. R. T. King, J. O. Stiegler, and G. M. Goodwin, "Relation Between Mechanical Properties and Microstructure in CRE Type 308 Weldments," *Weld. J. (Miami)* 53(7): 307-s–13-s (1974).
3. R. G. Berggren et al., "Structure and Elevated Temperature Properties of Type 308 Stainless Steel Weld Metal with Varying Ferrite Contents," *Weld. J. (Miami)* 57(6): 167-s–74-s (1978).
4. D. P. Edmonds, "Residual Elements Have Significant Effects on the Elevated-Temperature Properties of Austenitic Stainless Steel Welds," pp. 56–58 in *Properties of Austenitic Stainless Steels and Their Weld Metals (Influence of Slight Chemical Variations)*, American Society for Testing Materials, Philadelphia, 1979.
5. D. P. Edmonds, D. M. Vandergriff, and R. J. Gray, "Effect of Delta Ferrite Content on the Mechanical Properties of E308-16 Stainless Steel Weld Metal — III. Supplemental Studies," pp. 47–61 in *Properties of Steel Weldments for Elevated Temperature Pressure Containment Applications*, American Society of Mechanical Engineers, New York, 1978.
6. T. Takalo, N. Suutala, and T. Moisio, "Influence of Ferrite Content on Its Morphology in Some Austenitic Weld Metals," *Metall. Trans. A* 7A: 1591–92 (1976).
7. N. Suutala, T. Takalo, and T. Moisio, "The Relationship Between Solidification and Microstructure in Austenitic and Austenitic-Ferritic Stainless Steel Welds, *Metall. Trans. A* 7A: 512–14 (1979).

8. J. K. Lai et al., "Variations in Delta-Ferrite Content and Morphology in a Multipass Type 316 Weldment and Their Effect on Creep Rupture Properties," pp. 233–38 in *Welding and Fabrication in the Nuclear Industry*, British Nuclear Energy Society, London, 1979.
9. S. A. David, "Ferrite Morphology and Variations in Ferrite Content in Austenitic Stainless Steel Welds," *Weld. J. (Miami)* 60: 63-s–71-s (1981).
10. K. J. Irvine, T. Gladman, and F. B. Pickering, "The Strength of Austenitic Stainless Steels," *J. Iron Steel Inst., London* 207: 1017–28 (1969).
11. E. E. Bloom, *Effect of Titanium Additions on the Stress-Rupture Properties of Type 304 Stainless Steel*, ORNL/TM-1807, June 1967.
12. J. E. White and J. W. Freeman, "Metallurgical Principles Governing the Creep-Rupture Strength of Type 321 Stainless Steel Superheating Tubing with Limited Extension to Type 304 and Type 316 Austenitic Steels," *J. Eng. Power* 85: 119–67 (1963).
13. E. E. Bloom, J. M. Leitnaker, and J. O. Stiegler, "Effect of Neutron Irradiation on the Microstructure and Properties of Titanium-Stabilized Type 316 Stainless Steels," *Nucl. Technol.* 31: 232–43 (1976).
14. A. G. Allten, J.G.Y. Chow, and A. Simon, "Precipitation Hardening Austenitic Chromium-Nickel Steels Containing High Carbon and Phosphorus," *Trans. Am. Soc. Met.* 45: 948–72 (1954).
15. F. H. Froes, M.G.H. Wells, and B. R. Banerjee, "Influence of Phosphorus on the Nucleation of $M_{23}C_6$ Carbides in Austenitic Stainless Steels," *Met. Sci. J.* 2: 232–34 (1968).
16. K. J. Irvine, D. T. Llewellyn, and F. B. Pickering, "High-Strength Austenitic Stainless Steels," *J. Iron Steel Inst., London* 199: 153–75 (1961).
17. A. J. Rowcliffe and R. B. Nicholson, "Quenching Defects and Precipitation in a Phosphorus-Containing Austenitic Stainless Steel," *Acta Metall.* 20: 143–55 (1972).
18. G. Henry et al., "Influence de Faibles Additions de Bore sur la Resistance au Fluage et la Structure Micrographique D'aciers Derivant du Type 18-10," *Rev. Metall. (Paris)* 61: 1221–32 (1963).

19. G. Henry et al., "Orientation and Morphology of $M_{23}(BC)_6$ Precipitates in Austenite Grain Boundaries," pp. 666–67 in *Electron Microscopy 1974*, Australian Academy of Science, Canberra, A.C.T., Australia, 1974.

20. B. J. Thomas and G. Henry, "Boron in Austenitic Stainless Steels," pp. 80–105 in *Boron in Steels*, The Metallurgical Society of AIME, Warrendale, Pa., 1980.

21. M. O. Maline, "Sigma and 885°F Embrittlement of Chromium-Nickel Stainless Steel Weld Metals," *Weld. J. (Miami)* 46(6): 241-s–53-s (1967).

22. D. Hauser and J. A. Van Echo, "Effect of Delta Ferrite Content of E308-16 Stainless Steel Weld Metal II. Mechanical Property and Metallographic Studies," pp. 17–46 in *Properties of Steel Weldments for Elevated Temperature Pressure Containment Applications*, American Society of Mechanical Engineers, New York, 1978.

23. A. S. Grot and J. E. Spruiell, "Microstructural Stability of Titanium-Modified Type 316 and Type 321 Stainless Steel," *Metall. Trans. A* 6A: 2023–30 (1975).